Advanced Drug Delivery Reviews 105 (2016) 145–162

Contents lists available at ScienceDirect

Advanced Drug Delivery Reviews

journal homepage: www.elsevier.com/locate/addr

Interactions of graphene with mammalian cells: Molecular mechanisms and biomedical insights☆

Bo Zhang [a,1], Peng Wei [a,b,1], Zhixiang Zhou [c,1], Taotao Wei [a,*]

[a] National Laboratory of Biomacromolecules, Institute of Biophysics, Chinese Academy of Sciences, Beijing 100101, China
[b] University of Chinese Academy of Sciences, Beijing 100049, China
[c] College of Life Science and Bioengineering, Beijing University of Technology, Beijing 100124, China

ARTICLE INFO

Article history:
Received 14 March 2016
Received in revised form 18 August 2016
Accepted 22 August 2016
Available online 26 August 2016

Keywords:
Graphene
Lysosome
Mitochondria
Metabolism
Cancer therapy
Biomedicine
Interaction
Intracellular components

ABSTRACT

Carbon-based functional nanomaterials have attracted immense scientific interest from many disciplines and, due to their extraordinary properties, have offered tremendous potential in a diverse range of applications. Among the different carbon nanomaterials, graphene is one of the newest and is considered the most important. Graphene, a monolayer material composed of sp^2-hybridized carbon atoms hexagonally arranged in a two-dimensional structure, can be easily functionalized by chemical modification. Functionalized graphene and its derivatives have been used in diverse nano-biotechnological applications, such as in environmental engineering, biomedicine, and biotechnology. However, the prospective use of graphene-related materials in a biological context requires a detailed comprehension of these materials, which is essential for expanding their biomedical applications in the future. In recent years, the number of biological studies involving graphene-related nanomaterials has rapidly increased. These studies have documented the effects of the biological interactions between graphene-related materials and different organizational levels of living systems, ranging from biomolecules to animals. In the present review, we will summarize the recent progress in understanding mainly the interactions between graphene and cells. The impact of graphene on intracellular components, and especially the uptake and transport of graphene by cells, will be discussed in detail.

Contents

Abbreviations: ATP, adenosine triphosphate; CDDP, *cis*-diamminedichloroplatinum; DOX, doxorubicin; ETC, electron transfer chain; EGFR, epidermal growth factor receptors; ESR, electron spin resonance; EA, electron affinity; ECM, cell-extracellular matrix; FLG, few layer graphene; FADH, flavin adenine dinucleotide; FBS, fetal bovine serum; GM-CSF, granulocyte macrophage colony-stimulating factor; GO, graphene oxide; GNR, graphene nanoribbon; GONR, graphene-oxide nanoribbon; GONP, graphene-oxide nanoplatelet; GQD, graphene quantum dot; GO-NH_2, aminated GO; GO-PAM, poly(acrylamide)-functionalized GO; GO-PAA, poly(acrylic acid)-functionalized GO; GO-PEG, poly(ethylene glycol)-functionalized GO; GTPase, guanosine triphosphate hydrolase; HPV, human papillomavirus; HPS, human plasma serum; IFN, interferon; IgG, immunoglobulin G; IL, interleukin; LDH, lactate dehydrogenase; MCP, monocyte chemotactic protein; MIP, macrophage inflammatory protein; MMP, mitochondrial membrane potential; MD, molecular dynamics; NGO, nanographene; NADH, nicotinamide adenine dinucleotide; OXPHOS, oxidative phosphorylation; PEG, polyethylene glycol; Path-Net analyses, pathway analysis using network information algorithm; PCGO, protein-coated GO nanosheet; RANTES, regulated on activation, normal T cell expressed and secreted; ROS, reactive oxygen species; rGO, reduced graphene oxide; SILAC, Stable isotope labeling by amino acids in cell culture; TCA, tricarboxylic acid cycle; TEM, transmission electron microscopy; TGF, transforming growth factor; TLR, toll-like receptor; TNF, tumor necrosis factor.

☆ This review is part of the *Advanced Drug Delivery Reviews* theme issue on "Graphene-based materials in nanomedicine."

* Corresponding author.
E-mail address: weitt@moon.ibp.ac.cn (T. Wei).

[1] BZ, PW, and ZZ contributed equally to this work.

http://dx.doi.org/10.1016/j.addr.2016.08.009

1. Introduction

Graphene is a single layer of carbon packed in a hexagonal (honeycomb) lattice with carbon–carbon distances of 0.142 nm. It was first isolated by Andre Geim and Konstantin Novoselov, the 2010 laureates of the Nobel Prize in Physics, from its three-dimensional parent material, graphite [1]. Since then, this research area has exploded, producing a rapidly growing number of papers concerning graphene and graphene-related materials (Fig. 1) [2], including few layer graphene (FLGS), ultrathin graphite, graphene oxide (GO), reduced graphene oxide (rGO), and graphene nanosheets.

Graphene and graphene-related nanomaterials have attracted tremendous attention and research interest owing to their physical properties, such as their exceptionally large surface area, high electronic conductivity, good thermal stability, and excellent mechanical strength [2]. They have a wide range of potential applications in electronics and optoelectronics [3,4], energy conversion [5,6] and storage [7], catalysis [8,9], and environmental applications [10]. Recently, the biological applications of graphene and graphene-related nanomaterials have attracted attention in the scientific community based on their great potential for use in bio-imaging [11,12], cancer theragnosis [13–15], gene delivery [16], tissue engineering [17,18], biosensing [19], DNA sequencing [20], and drug delivery [21–23]. Several reviews have summarized the applications of graphene-related nanomaterials in biology and medicine [24–29].

Graphene-related nanomaterials have now been developed in many different forms in terms of their shapes, sizes, and surface modifications, which endow them with versatile physical, chemical, and biomedical characteristics. In vitro cytotoxicological investigations are required in order to develop graphene-related biomedical materials, and systematic evaluations of the biocompatibility of graphene-related materials are essential before their application in vivo. Since 2008, numerous studies have investigated the nanotoxicology and biocompatibility of graphene-related materials, and several reviews have been published [25,30,31]. However, how graphene-related materials perform these biomedical effects is still not clearly summarized; there is still a lack of a systematic review on the interaction between graphene and biological systems at the cellular level. In this paper, we aim to summarize the recent research advances in this field. We begin by reviewing three systems biology-based studies on the biological effects of graphene in different cell types. By assessing the omics data with Gene Ontology analyses, Path-Net analyses, and other bioinformatics approaches, we show that graphene and its derivatives impact the cell components, especially the plasma membrane and the membrane organelles, and interfere with the cellular metabolism. Next, we discuss how the structure and function of the plasma membrane, lysosomes, mitochondria, and other cellular components are affected by graphene. Considering the application potential of graphene as drug or gene carriers, we discuss in detail the interactions between graphene and certain types of cells, including hemocytes, blood vessel endothelial cells, macrophages, cancer cells, and stem cells.

2. Systems biology-based analyses of the biological effects of graphene

Systems biology approaches based on integrated omics and bioinformatics analyses have undergone rapidly and could be used as powerful tools to explore the interactions between nanomaterials and biosystems. Chatterjee and coworkers profiled the gene expression at the mRNA level in HepG2 hepatoma cells treated with graphene oxide (GO). The differential gene expression of a normalized microarray analysis revealed that 1224 genes were induced or repressed by more than 1.5-fold under GO treatment. The Gene Ontology analysis indicated that genes related to the regulation of cell growth and apoptosis, the

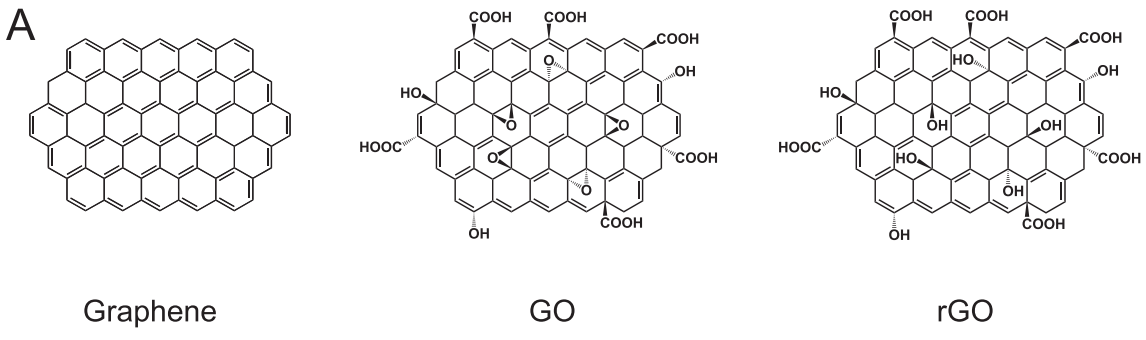

Fig. 1. Structure of graphene, graphene oxide (GO) and reduced graphene oxide (rGO) [2].

response to oxygen levels and hypoxia, and metabolic processes were regulated as a result of GO treatment [32].

Zhou and coworkers also investigated the effects of GO on MDA-MB-231 breast cancer cells by evaluating the gene expression at the protein level. Using the SILAC (stable isotope labeling by amino acids in cell culture) method, they quantified the protein expression in both breast cancer cells and non-cancerous cells, identifying and quantifying a total of 2254 cellular proteins expressed in breast cancer cells (Fig. 2). Based on a cutoff value of 1.2, 168 proteins were found to be up-regulated and 685 proteins were down-regulated by GO. Gene Ontology and Path-Net analyses indicated that multiple proteins involved in metabolic processes, the regulation of cell growth, and apoptosis were influenced by GO treatment. A further bioinformatics analysis suggested that proteins related to energy metabolism, particularly oxidative phosphorylation (OXPHOS) and tricarboxylic acid cycle-related proteins, were widely down-regulated in MDA-MB-231 cells treated with GO; this may explain the impaired OXPHOS and decreased ATP generation observed in that study [33].

Graphene-related nanomaterials also modulate the expression of miRNAs. Li and coworkers profiled the expression of miRNA in GLC-82 lung cancer cells exposed to GO and found that 653 miRNAs were differentially expressed; among them, 628 miRNAs were up-regulated, and 25 miRNAs were down-regulated. Therefore, the expression patterns of miRNAs in GLC-82 cells were globally influenced by GO. A Gene Ontology

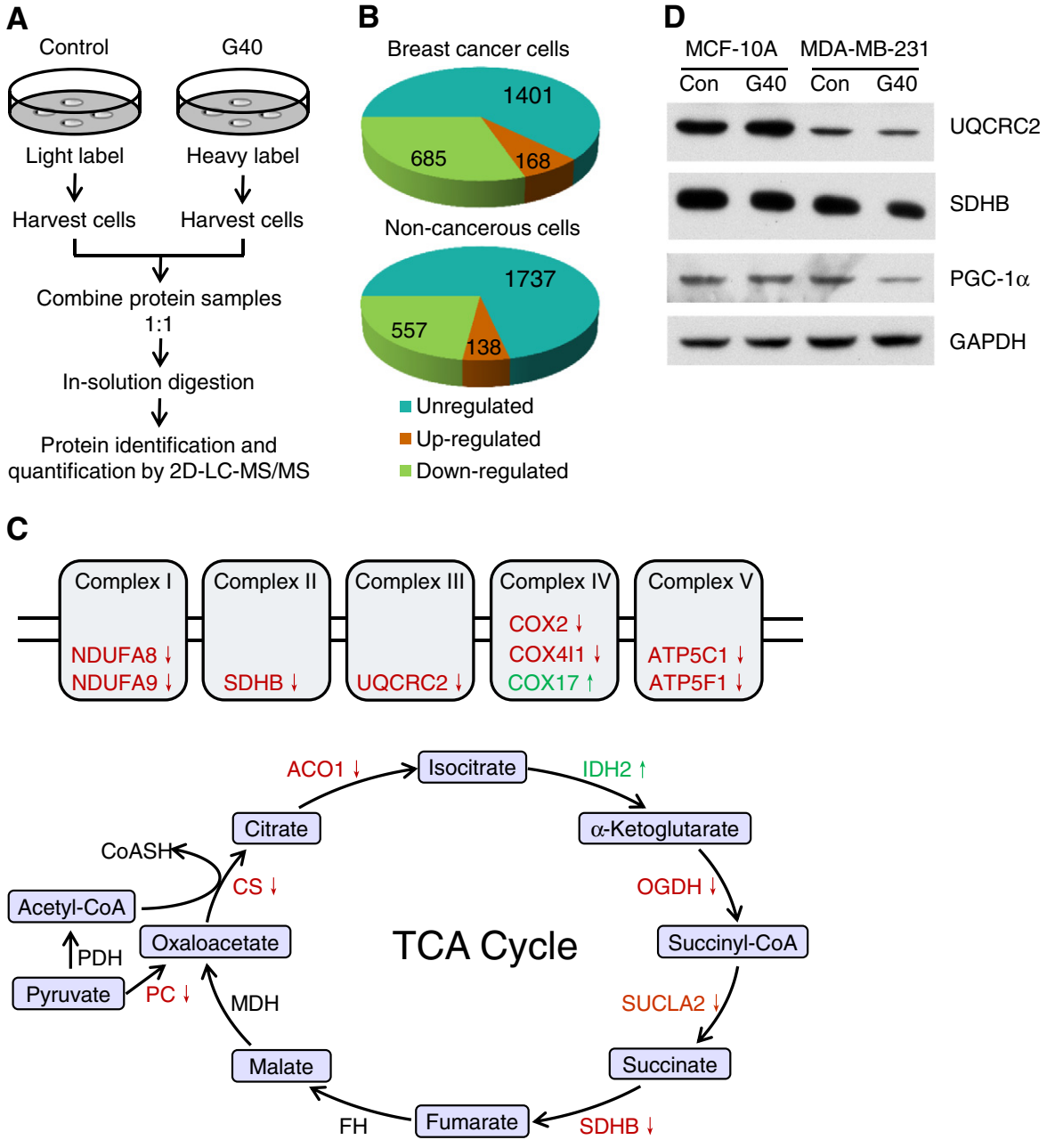

Fig. 2. Systems biology analysis of differently expressed genes upon PEG-GO exposure. (A) Schematic representation of SILAC strategy coupled with 2D-LC-MS/MS. MDA-MB-231 breast cancer cells and MCF-10 A non-cancerous mammary epithelial cells were incubated with (heavy label) or without (light label) 40 μg/ml PEG-GO for 24 h and followed by subsequent analysis. (B) Pie chart displaying the overall protein expression regulation of cells upon PEG-GO treatment with a 1.2-fold cutoff. (C) Schematic of the TCA cycle pathway and mitochondrial complexes-related protein expression in MDA-MB-231 cells treated with PEG-GO. Red arrows indicate the protein down-regulations and the green arrows indicate the protein up-regulations analyzed using SILAC-based proteomics. (D) Expression profile of PGC-1α, SDHB (Complex II), and UQCRC2 (Complex III) in MDA-MB-231 and MCF-10 A cells. Cells were incubated with 40 μg/ml PEG-GO for 24 h and followed by western blotting analysis. Image adapted from Reference [33] with permission, copyright © Elsevier B.V. 2014.

analysis provided 89 up-regulated and 12 down-regulated gene ontology terms classified into several categories, including the regulation of cell growth and apoptosis, inflammation, metabolic processes, and development [34].

In these three research works, genes whose expression profiles were significantly altered in GO samples comparing to normal samples have been identified. The relationship among those differentially expressed genes and how they work coordinately as a molecular group have also been further analyzed, which construct or imply us the GO–cell interactions, GO-organelle interactions, and protein–protein interactions. The results indicated that graphene and its derivatives affect the cellular components, especially the plasma membrane, cytoskeleton, and the membrane organelles (including the mitochondrion, lysosome, and nucleus). GO treatment alters the metabolic processes, impacts cell growth, and induces apoptosis at higher concentrations. We will review these biological effects in detail below.

3. Interactions between graphene and the plasma membrane

Graphene and graphene-related nanomaterials have attracted great interest in nanomedicine due to their intrinsic properties. Interactions at the interface of graphene and mammalian cells must be considered in studies assessing the use of graphene in biomedical applications; some studies have shown that the internalization of graphene is a mechanism that can lead to cell intoxication, while other studies have shown that graphene internalization can transport therapeutic agents intracellularly without ensuing damage. Thus, graphene internalization may cause completely different effects on different cell types. Researchers should carefully consider the chemical and physical properties of graphene as well as the cellular context when they design graphene-based nanomaterials [35]. Here, we summarize the recent progress in understanding the internalization of graphene and graphene-related nanomaterials by mammalian cells, the impact on the integrity of the plasma membrane, and the interaction between graphene and biomolecules.

3.1. Internalization of graphene across the plasma membrane

Like other nano-sized substances, graphene and graphene-related nanomaterials are primarily internalized into cells via endocytosis, which can be subdivided into four categories: clathrin-mediated endocytosis, caveolae-mediated endocytosis, macropinocytosis, and phagocytosis. Notably, the internalization of graphene into cells is known to be related to the cell type. Linares and coworkers investigated the impact of eight inhibitors (colchicine, wortmannin, amiloride, cytochalasin B, cytochalasin D, genistein, phenylarsine oxide, and chlorpromazine) that specifically affect different endocytotic mechanisms on the cellular uptake of GO nanosheets by three different cell types (Saos-2 osteoblasts, HepG2 hepatoma cells, and RAW-264.7 macrophages). They found that macropinocytosis seems to be a general internalization process in the three cell lines analyzed. In addition, GO can enter Saos-2 cells through microtubule-dependent pathways and HepG2 and RAW-264.7 cells through clathrin-dependent mechanisms [36].

The internalization of graphene-related nanomaterials into cells is strongly influenced by the particle size. A study with protein-coated GO nanosheets showed that small GO enter cells primarily through clathrin-mediated endocytosis; increasing the size of GO enhances their phagocytotic uptake [37]. Surface chemistry also influences the internalization of graphene-related materials [38,39]. Chatterjee and coworkers reported that GO could be internalized by HepG2 cells; on the contrary, reduced GO (rGO), which is much more hydrophobic in comparison with GO, was found to mostly adsorb onto the cell surface without internalization [32]. However, in certain types of cells, both GO, and rGO flakes of different sizes could be taken up effectively by cells via the endocytic pathway [40].

Scientists could manipulate the internalization of graphene via modulation of the particle size and surface chemistry. The internalization of graphene nanoribbon (GNR) derived from the longitudinal unzipping carbon nanotubes has been investigated systematically in different cell types [39,41]. Chowdhury and coworkers show that functionalized GNR activate epidermal growth factor receptors (EGFRs). This activation generates a predominantly dynamin-dependent macropinocytosis-like response and results in significant GNR uptake into cells with high EGFR expression. Cells with an integrated human papillomavirus (HPV) genome also show increased uptake due to the modulation of the activated EGFR by the viral protein E5. Thus, this cell-specific uptake of GNR can be exploited to achieve significantly enhanced drug efficacies even in drug-resistant cells. These results have implications for the development of active targeting and delivery agents for use in the diagnosis and treatment of pathologies [42]. For example, functionalized GNR could be used as an efficient agent for delivery of anti-tumor drug lucanthone into glioblastoma multiforme (GBM) cells targeting base excision repair enzyme apurinic endonuclease-1 [43].

The dynamics of the internalization of graphene can be traced by cell imaging-based experiments and computational simulation-based in silico approaches. Li and coworkers investigated the interactions between graphene and model lipid bilayers by combining coarse-grained molecular dynamics (MD), all-atom molecular dynamics, analytical modeling, confocal fluorescence imaging, and electron microscopic imaging. The imaging experiments showed edge-first uptake and the complete internalization of a range of graphene and few layer graphene (FLG) samples of 0.5- to 10-μm in the lateral dimension. Computational simulations indicated that the entry of graphene and FLG is initiated at corners or asperities, which are abundant along the irregular edges of fabricated graphene materials. Local piercing by these sharp protrusions initiates membrane propagation along the extended graphene edge, thereby avoiding the high energy barrier. These findings provide a fundamental understanding of interactions at the interface of two-dimensional nanostructures and biological systems (Fig. 3) [44].

3.2. Impacts on the dynamics and integrity of the plasma membrane

Although low concentrations of graphene and graphene-related nanomaterials show little or no toxicity in mammalian cells, high concentrations of graphene alter the dynamics and integrity of the plasma membrane during their internalization, and induce cell death. Liao and coworkers investigated the effects of graphene on human erythrocytes and found that nano-sized graphene (350 nm) could induce severe hemolysis compared to micro-sized (3 μm) graphene sheets [45]. They suggested that the serious membrane disruption by nano-sized graphene might be attributed to the strong electrostatic interactions between the graphene surface and the lipid bilayer of the erythrocyte membrane. By contrast, the relatively low toxicity of micro-sized graphene sheets may have been due to their lower overall surface areas.

Graphene also impacts the integrity of the plasma membrane in other mammalian cells. Li and coworkers reported that exposure of GLC-82 lung cancer cells to GO for 48 h induced the redistribution of cytoplasmic lactate dehydrogenase (LDH), suggesting the significant loss of plasma membrane integrity [34]. Similar results have been observed in other cell types, including MCF-7 breast cancer cells, Panc-1 pancreatic cancer cells [46], and MDA-MB-231 breast cancer cells [47], implying that the exposure of cells to high concentrations of graphene damages the membrane integrity. Accordingly, blocking the internalization of graphene with endocytosis inhibitors has been shown to attenuate the graphene-induced plasma membrane damage [32]. Lammel and coworkers observed the impact of graphene on the ultrastructure of the plasma membrane and found that nano-sized graphene penetrates the plasma membrane (Fig. 4). They showed that at the site of interaction between the graphene nanoplatelet and the plasma membrane, membrane invagination and some disruption of the plasma membrane occur. At

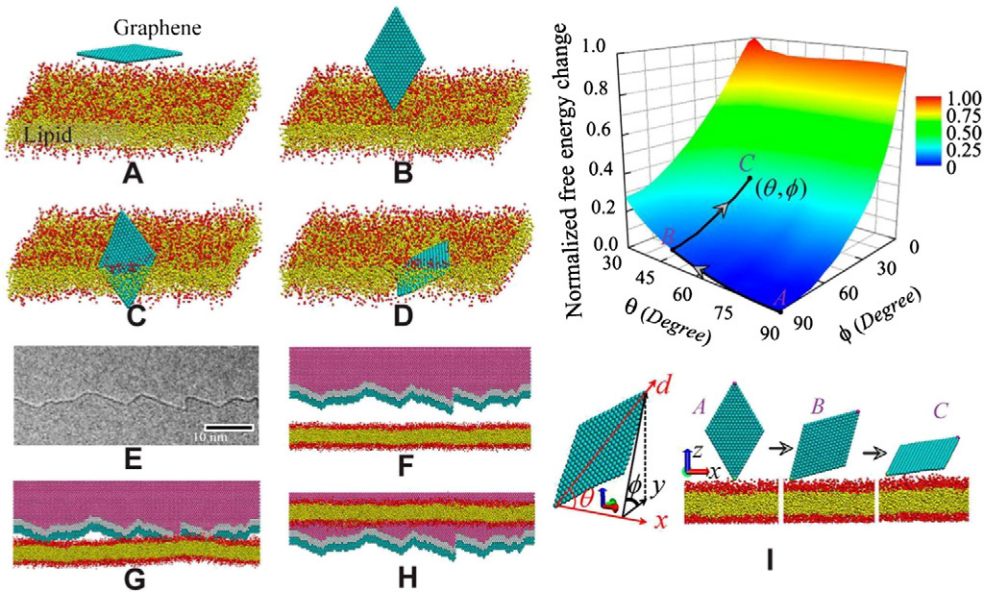

Fig. 3. Dynamics of the interaction between graphene and membrane systems. (A–H) Coarse-grained molecular dynamics simulations of interactions between a lipid bilayer. (A–D) and (F–H) are time sequences; (E) is an experimental graphene edge structure. (I) The normalized free energy of the system as a function of the graphene orientation when one of the sharpest corners is fixed at a distance of 0.5 nm above the bilayer. The results of the molecular dynamics simulations indicated that the entry of graphene across the membrane systems is initiated at corners or asperities. Local piercing by these sharp protrusions initiates membrane propagation along the extended graphene edge, thereby avoiding the high energy barrier. Image adapted from Reference [44] with permission, copyright © HighWire Press, Inc. 2014.

graphene nanoplatelet concentrations of 8 μg/ml and lower, only a portion of the cell surface interacted with the graphene platelets. While the micro-sized graphene platelets were retained by the microvilli, the nano-sized platelets were deposited onto the microvilli-free plasma membrane domains [48].

Graphene also influences the membrane integrity and dynamics via indirect mechanisms. The in vitro experiments by Xu and coworkers revealed that pristine GO could impair cell membrane integrity and functions by regulation of membrane- and cytoskeleton-associated genes, including Actg2, Myosin, Tubb2a, and Nebulin [49]. Matesanz

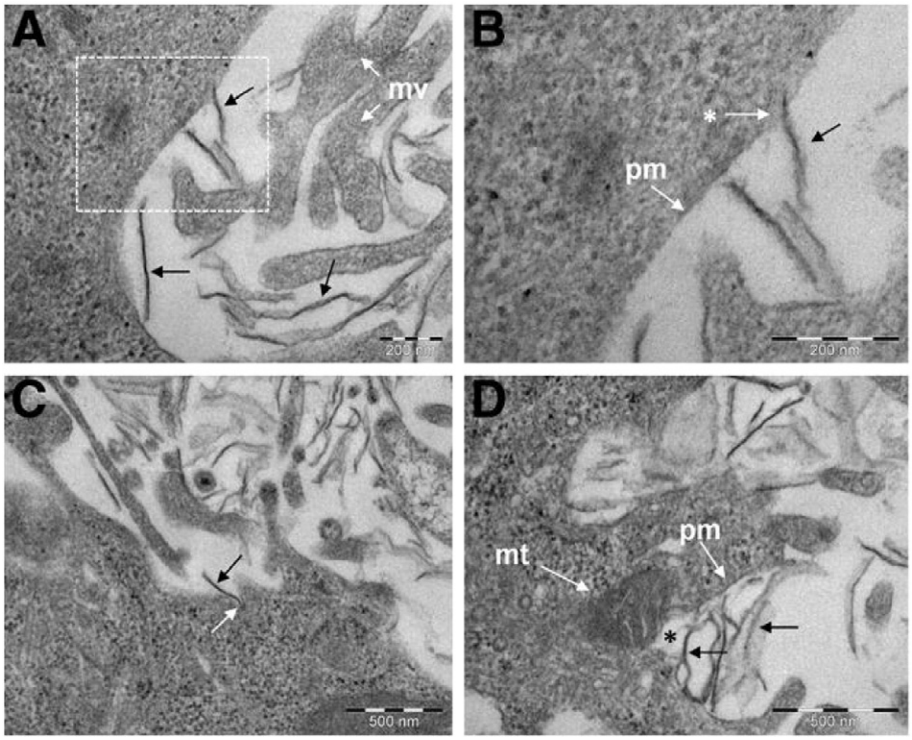

Fig. 4. Interaction between GO nanoplatelets with the plasma membrane of HepG2 cells. (A) SEM micrograph showing the interaction of GO nanoplatelets (exemplarily indicated by black arrows) with the plasma membrane (pm) and microvilli (mv). (B) SEM micrographs showing the boxed-in area in A at higher magnification. GO nanoplatelet penetrating the plasma membrane (arrow with white asterisk). (C) Membrane invagination (white arrow) at the site of interaction of a GO nanoplatelet (black arrow) with the plasma membrane. (D) Disruption of the plasma membrane (black asterisk) at the site of interaction with GO nanoplatelets (exemplarily indicated by black arrows). Scale bars represent 200 nm in A and B, and 500 nm in (C) and (D). Black arrows exemplarily indicate GO nanoplatelets. mt: mitochondrion, pm: plasma membrane, mv: microvilli. Image adapted from Reference [48] with permission, copyright © BioMed Central Ltd. 2013.

and coworkers also demonstrate that, after internalization, GO nanosheets are localized on F-actin filaments and thus induce cell cycle alterations, apoptosis, and oxidative stress in mammalian cells [50].

The size of graphene-related materials influences their impact on plasma membrane significantly. Akhavan and coworkers synthesized reduced graphene-oxide nanoplatelets (rGONPs) and evaluated the size-dependent toxicity on the mesenchymal stem cells (MSC). The cell viability test showed significant cell destructions by 1.0 μg/mL rGONPs with average lateral dimensions (ALDs) of 11 ± 4 nm, while the rGO sheets with ALDs of 3.8 ± 0.4 μm could exhibit a significant cytotoxic effect only at high concentration of 100 μg/mL after 1 h exposure time [51].

The shape of the nano-sized graphene impacts their effects on the integrity of cell membranes. Chng and coworkers compared the cytotoxicity of graphene-oxide nanoribbons (GONRs) and graphene-oxide nanoplatelets (GONPs). In vitro assessments revealed that the GONRs exhibited a much stronger cytotoxicity over the GONPs. In comparison with GONPs derived from graphite using Hummer's method, GONRs derived from the longitudinal unzipping carbon nanotubes are often larger, more oxidized, and differently shaped. The high aspect ratio and the greater amount of carbonyl groups of GONR might be the related with its higher cytotoxicity [52].

Surface chemistry also influences the graphene–membrane interactions. By combining large-scale computational simulations, theoretical analyses, and experimental investigations, Mao and coworkers evaluated the interactions between graphene nanosheets with varying degrees of oxidation and a model lipid bilayer membrane. They found that the perturbation degree of the lipid bilayer membrane increases with increasing the edge length of nanosheet at each oxidization degree. With the graphene oxidization degree increased, the membrane perturbation becomes more irregular while the perturbation range becomes wider. Graphene nanosheets tend to pierce the membrane and to take a configuration vertical to the membrane with the increase of oxidization degree. From an energy perspective, the energy due to the repulsion between lipid tails and oxidized graphene beads can be significantly reduced when the oxidized basal plane deviates away from the center of bilayer membrane. However, the pierced membrane losses its integrity and presents a large scale of irregular perturbation, corroborating the observation of the thickness field. These results imply that a graphene nanosheet with larger size and higher oxidization degree may lead to stronger cytotoxicity [35]. These data not only provide new mechanistic insight into how the cellular internalization of graphene-based nanomaterials occurs but also offer a fundamental understanding of the physicochemical properties of these materials, which can be precisely tailored for safer biomedical applications.

4. Impact of graphene on intracellular organelles

After its internalization, graphene is entrapped within the endosome/lysosome system. Using the endosome/lysosome as the basement of intracellular interactions, graphene interacts with other intracellular organelles and machineries and triggers cellular responses. Here, we summarize the impact of graphene on important intracellular organelles and machineries, including lysosomes, mitochondria, nuclei, and the cytoskeleton system, which will be helpful for the understanding of the bio-effects of graphene at the cellular level.

4.1. Impact on lysosome-related organelles

As mentioned above, graphene is mainly internalized by cells via endocytosis. Thus, the endosome/lysosome system is pivotal to the intracellular transportation and entrapment of graphene. Li and coworkers reported that GO and GO nanoassemblies are mainly distributed in acidic lysosomes of mouse embryonic fibroblasts (MEF) after their internalization [53]. Similar results have also been reported in 4T1 breast cancer cells by Chen [54]. The conjugation of a bulky fluorophore to graphene may alter its surface chemistry and thereby interfere with its internalization and translocation. However, graphene can be visualized under a fluorescence microscope by quenching the emission from a dye [55]. To detect the presence of graphene in the lysosomes, MDA-MB-231 breast cancer cells were stained with a lysosome-specific fluorescence probe. The results based on a 3D-reconstruction of confocal images clearly indicated that the fluorescence of the lysosomes could be partially quenched by graphene, suggesting that graphene nanoparticles were near or inside the lysosomes [56].

Graphene nanostructures with lysosome-targeting properties have shown potential applications in biomedicine, especially as drug carriers. Zeng and coworkers constructed a graphene-based, lysosome-targeting delivery system in which nanographene (NGO, 20–40 nm) particles were modified by covalent functionalization with a linear chain of PEG. The photosensitizer molecule Chlorin e6 (Ce6) was loaded onto the NGO-PEG particles via π-π stacking and hydrophobic interactions. By using this nanoplatform, a photosensitizer could be selectively translocated into the lysosomes, which significantly enhanced the efficacy of photodynamic therapy [57].

The influence of graphene on lysosomes is concentration dependent. Low concentrations of graphene shows little to no effects on the integrity of the lysosomal membrane and thus do not influence the cell viability. However, high concentrations of graphene cause lysosomal membrane permeabilization, which results in cell death via different pathways, including lysosome/mitochondria-dependent apoptosis [58], lysosome-dependent necrosis, and lysosome-dependent autophagic cell death. Recently, the impact of graphene on the autophagic machinery has attracted increased attention. Autophagy and autophagic cell death have been recently recognized as important lysosome-based cell death pathways, and autophagosome accumulation has been found to be associated with exposure to various nanoparticles. However, the underlying mechanisms are still uncertain because autophagosome accumulation can result from autophagy induction and/or an autophagy blockade. GO can induce autophagosome accumulation and the conversion of LC3-I to LC3-II, as evidenced by the inhibitory effect of graphene oxides on the degradation of the p62 protein, an autophagic substrate. Further analyses of lysosomes revealed that graphene oxides accumulate in macrophage lysosomes and lead to lysosome membrane destabilization, which indicates reduced autophagic degradation [59]. As the effects of GO on cell lysosomes and autophagy reveal a potentially toxic mechanism, caution is recommended in the utilization of GO.

4.2. Impact on mitochondria

Mitochondria function as signaling hubs that are essential for maintaining aspects of physiology, such as the cellular energy balance, metabolism, and the modulation of calcium signaling. The mitochondria also define the cellular redox balance, regulate important biosynthetic pathways, and act as sensors and amplifiers of cellular damage. Thus, the mitochondria play crucial roles in the induction of cell death. Recently, we and other groups have found that graphene and graphene-related nanomaterials can interact with the mitochondria, modulating their morphology and function. Because the mitochondria are closely related to the survival, differentiation, and death of cells, exploring the mechanisms that underlie the interactions between graphene and mitochondria will be of great value.

4.2.1. Decrease of membrane potential

Internalized graphene is mainly entrapped within the lysosome. However, a small proportion of graphene can relocate to the cytosol, where it can interact with the mitochondria, as evidenced by the fluorescence quenching assay [56]. Similar results were also reported by Li and coworkers, who used transmission electron microscopy (TEM) to observe the accumulation of GO within the cytosol and mitochondria [34].

Mitochondria are the major sources of intracellular ATP, and the mitochondrial membrane potential (MMP) is crucial to ATP synthesis. The MMP decreases in response to graphene treatment. Lammel and coworkers reported that exposing cells to GO results in the perturbation of the mitochondrial structure and function, as characterized by a decrease in the mitochondrial membrane potential and the dysregulation of mitochondrial Ca^{2+} homeostasis [48]. Similar to nano-sized GO, pristine graphene [32] and graphene quantum dots [60] also caused time- and concentration-dependent decreases in the mitochondrial membrane potential.

The maintenance of the MMP is dependent on the oxidation of various substances catalyzed by electron transfer chain (ETC) complexes: complex I and complex II (succinate dehydrogenase) catalyze the transfer of electrons from NADH and FADH to coenzyme Q, respectively. Coenzyme Q then transfers electrons to complex III, which passes them to cytochrome *c*, which in turn donates electrons to complex IV. The passage of electrons between the donors and acceptors generates a proton gradient across the mitochondrial membrane, which complex V utilizes for ATP synthesis. Through a combination of confocal microscopy, flow cytometry, and enzymatic activity assays, Zhou and coworkers provided direct evidence that exposing cells to graphene leads to the direct inhibition of the ETC complexes I, II, III, and IV, resulting in the depolarization of mitochondria and the consequent impairment of ATP production (Fig. 5) [56].

4.2.2. Induction of ROS generation

Mitochondrial depolarization is also associated with mitochondrial dysfunction and the overproduction of reactive oxygen species (ROS) [48,61]. These processes have been suggested to be the main mechanisms underlying graphene toxicity in mammalian cells [62]. Li and coworkers found that pristine graphene causes a decrease in the MMP and, consequently, increased levels of intracellular ROS, which activate the mitochondria-dependent apoptotic pathway. These findings were evidenced by the permeablization of the mitochondrial outer membrane, the redistribution of mitochondrial cytochrome *c*, and the activation of caspases, which ultimately resulted in cell death [58].

The mechanisms underlying the graphene-induced decrease in the membrane potential, the impairment of ATP production, and the overproduction of ROS have been partially explored by several groups. Duch and coworkers suggested that GO might act as an electron donor, which increases the supply of electrons to complexes I and II of the electron transport chain (ETC) and accelerates the generation of ROS as a byproduct of mitochondrial respiration. However, the increase in oxygen consumption was not induced by treatment with pristine graphene, suggesting that the production of ROS by electron donation depends on the chemical characteristics of graphene [63]. By using the nematode as a model system, Zhang and coworkers suggested that GO triggers the overproduction of hydroxyl radicals and the formation of oxidizing cytochrome *c* intermediates, which are responsible for the oxidative stress [64]. They further compared the effects of GO with different degrees of oxidation on the production of ROS in mammalian cells, finding that GO stimulated a dramatic enhancement of ROS production and that GO particles with less oxidation produced higher levels of ROS. The results of electron spin resonance (ESR) spectrometry showed that lower degrees of GO oxidation were strongly associated with greater indirect oxidative damage through facilitating H_2O_2 decomposition into hydroxyl radicals as well as with higher direct oxidative abilities on cells. The theoretical simulation revealed that carboxyl groups and the sizes of aromatic domains in nanosheets had critical effects on the energy barrier of the H_2O_2 decomposition reaction [65].

The ability of graphene to induce ROS production is also related to its size [66]. By combining ESR spectrometry and theoretical calculations, Zhou and coworkers found that the size of graphene determines its electron affinity (EA) values. Theoretical calculations indicated that the size of a graphene sheet correlates with its ability to accept electrons. Graphene sheets with diameters greater than 6.7 nm are stronger electron acceptors than 4Fe4S iron–sulfur clusters, the reduction of which may be inhibited by these larger graphene sheets. The turning points at which graphene becomes an inhibitor of the reduction of Fe-porphyrin, 2Fe2S, and 3Fe4S are 1.2 nm, 2.9 nm, and 5.6 nm, respectively. The results of ESR indicated that nano-sized graphene alters the electronic distribution state, which may be due to the inhibitory effects of graphene on the reduction of three-valent iron ions to two-valent iron ions via the disruption of electron transfer [56]. Bypassing the electron transport chain by graphene impairs not only ATP production but also ROS overproduction.

Although size of the GO sheet plays a role, the functional group density on the GO sheet is one of the key components in ROS generation. Das and coworkers systematically investigated the toxicity of GO and rGO using an in vitro cell culture model system. They found GO is more toxic than rGO of same size. GO and rGO induce significant increases in both intercellular ROS levels and mRNA levels of HO1 and TrxR, two key genes involved in redox signaling. Such observations support the hypothesis that oxidative stress mediates the cellular toxicity of GO. Oxidative stress-induced cytotoxicity reduces with a decreasing extent of oxygen functional group density on the rGO surface, suggesting that it is possible to minimize the toxicity of GO and unravel its wide range of biomedical applications by controlling the GO reduction and maintaining the solubility [67].

Mitochondria are regarded as the major source of ROS generation; however, other cellular components are also involved. Horváth and coworkers evaluated the toxicity of GO and rGO in A549 human lung cancer cells and RAW 264.7 macrophages and found that cells treated with 0.0125–12.5 μg/cm^2 of GO or rGO for 5 days showed a dose-dependent cytotoxicity, which was due to the generation of ROS via the interaction of the nanomaterial with the cell surface during the initial phase of the exposure [40].

4.2.3. Remodeling of cellular energy metabolism

Cell survival and growth depend on metabolic pathways that produce energy, precursors for macromolecular synthesis, and substrates for other essential cellular functions. However, when cells face a considerable metabolic challenge, they may drastically adjust their utilization of many different metabolic pathways. For example, normal cells show active mitochondrial respiratory function and use oxidative phosphorylation (OXPHOS) as the main route to generate ATP. By contrast, cancer cells often exhibit an increased rate of glycolysis even in the presence of high O_2 concentrations. This phenomenon of "active aerobic glycolysis" is known as the Warburg effect, which is regarded as an important

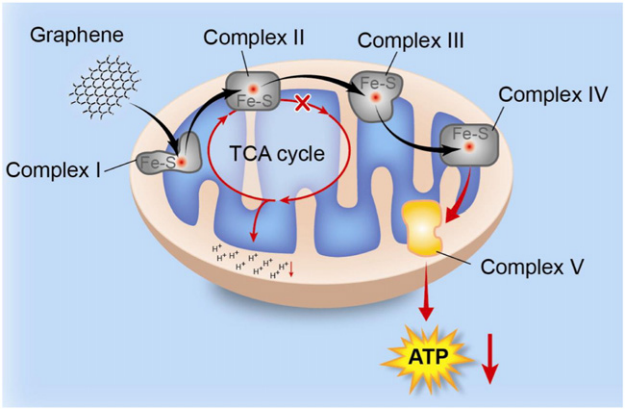

Fig. 5. The impairment of the mitochondrial energy production by graphene. Graphene directly inhibits the activity of electron transfer chain complexes by disturbing electron transfer. This leads to decreased mitochondrial membrane potential and reduced ATP synthesis. Image adapted from Reference [56] with permission, copyright © Elsevier B.V. 2014.

hallmark of cancer. Recently, Zhou and coworkers reported that GO inhibited mitochondrial OXPHOS in breast cancer cell lines. More importantly, GO had no apparent effect on the mitochondrial OXPHOS in non-cancerous mammary epithelial cells. Unlike OXPHOS, glycolysis in breast cancer cells was not affected by GO exposure and thus can partially compensate for the impaired OXPHOS in order to maintain essential ATP production [33]. Hu and coworkers investigated the impact of GO on the cellular metabolic profiles. A metabolomics analysis revealed significant differences between the control and GO-treated cells: the metabolisms of alkanes, lysine, octadecadienoic acid, and valine were associated with GO-induced ROS production and could be considered as new biomarkers of ROS. These authors also suggested that the GO-induced cytotoxicity involved the inhibition of fatty acid, amino acid, and small molecule acid metabolisms [61].

To explore the mechanism underlying alterations to cell metabolism, Zhou and coworkers analyzed the effects of GO on protein expression. By using a SILAC-based quantitative proteomics approach, they found that GO down-regulated the expression of multiple mitochondrial OXPHOS-related proteins, including NDUFA8, NDUFA9 (Complex I), SDHB (Complex II), UQCRC2 (Complex III), COX2, COX4I1 (Complex IV), ATP5C1, ATP5F1 (Complex V), and multiple enzymes involved in the TCA cycle, in breast cancer cells but not in non-cancerous cells. Therefore, they hypothesized that GO remodels the metabolisms of breast cancer cell lines by regulating pathways involved in energy metabolism [33].

4.3. Impact on other cellular components

Jin and coworkers reported that GO could enter A549 lung cancer cells and located within the cytoplasm and nucleus [68]. Similar results were also obtained in human dermal fibroblasts (HDF) [69]. Based on this cytoplasm-nucleus shuttle effect, graphene-derived nanomaterials might be used as carriers for drugs and genes. Wang and coworkers reported that graphene quantum dots (GQDs) could efficiently deliver doxorubicin (DOX) to the nucleus through DOX/GQD conjugates, which could increase the nuclear uptake of DOX, and thus enhance the cytotoxicity of DOX in drug-resistant cancer cells [70]. Chen and coworkers also reported that *cis*-diaminedichloroplatinum (CDDP) conjugated with GO could induce the nuclear import of CDDP effectively. In this process, importin-alpha/beta may play a critical role in the nuclear import of CDDP [71]. Probably these conjugates assume different cellular and nuclear internalization pathways comparing to free drugs.

Cytoskeleton is another key cellular component interacts with graphene and graphene-related nanomaterials. Matesanz and coworkers reported that GO nanosheets are localized on F-actin filaments of Saos-2 osteoblasts after their internalization, and thus impact cell cycle and cell death via a cytoskeleton-dependent manner [50]. Zhou and coworkers observed the impact of GO on the dynamics of cytoskeleton assembly in metastatic MDA-MB-231 breast cancer cells, and found that expose to GO leads to the disruption of F-actin cytoskeletal assembly within the lamellipodia and thus impaired cell migration (Fig. 6). By analyzing the expression of cytoskeleton-related genes, they found that two small GTPases involved in F-actin cytoskeleton assembly, Rac1 and RhoA, were down-regulated in MDA-MB-231 cells upon PEG-GO exposure [56]. Thus, graphene and graphene-related nanomaterials might influence the cytoskeleton via both direct and indirect mechanisms. Overall, these combined data delineated the molecular mechanisms underlying the in vivo and in vitro biological behaviors of graphene.

5. Biological effects of graphene on certain types of cells

The applications of graphene in biomedical fields have prompted substantial interest. Graphene substances that are usually functionalized have been designed to target different types of cells, including hemocytes, endothelial cells, phagocytes, and cancer cells. Therefore, it is essential to understand the interactions between graphene and these particular types of cells.

5.1. Biological effects on cells of the circulatory system

Graphene and graphene-related nanomaterials may enter the bloodstream and interact with blood components following their administration intended for biomedical purposes. The surface chemistry determines the hemocompatibility of graphene. For example, GO sheets elicited strong aggregatory response in platelets, while rGO was significantly less effective in aggregating platelets [72]. Once introduced into systemic circulation, graphene encounters various biomolecules and interacts with the cells of the circulatory system. This interaction alters

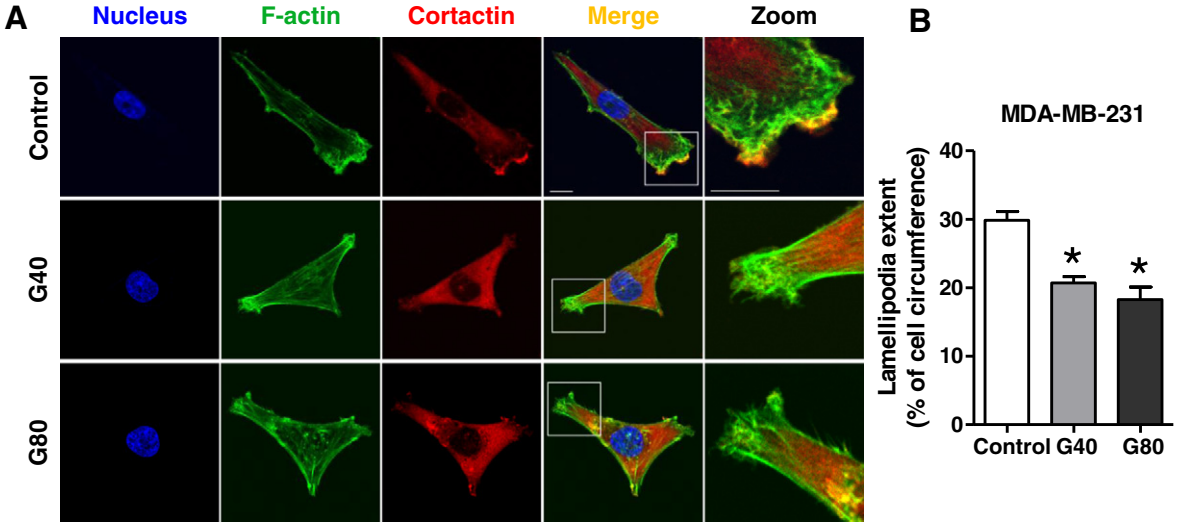

Fig. 6. Impairment of F-actin assembly by PEG-GO nanosheets in breast cancer cells. (A) MDA-MB-231 cells were seeded on cover slips, exposed to 40 or 80 μg/ml PEG-GO for 24 h and then stained with Alexa-Fluor 488-labeled phalloidin for F-actin (green), an antibody against cortactin (red) and DAPI for nuclei (blue). Scale bar, 5 μm. (B) Lamellipodia extents at cell edges were quantified as a percentage of the cell circumference on 50 randomly selected cells in each group. Values represent the means ± SEM, $^*p < 0.05$. Image adapted from reference [33] with permission, copyright © Elsevier B.V. 2014.

the surface properties of graphene and impacts the hemocompatibility of graphene.

5.1.1. Formation of the protein corona

It has been well established that when nanomaterials interact with biological systems, biomolecules, particularly proteins, attach to their surfaces to form a complex between the nanoparticle surface and the proteins called corona. The protein corona is a key concept in nanomedicine and nanotoxicology because it provides a biomolecular identity for nanomaterials in a biological environment. Thus, the interaction of a biological system with a nanomaterial depends on the composition of the protein layer rather than the surface characteristics of the nanomaterial itself. However, understanding the protein–graphene interaction of the corona and its influence on cellular responses is a challenging task at the nano-bio interface [73].

The bloodstream contains abundant protein molecules. Graphene can spontaneously and rapidly interact with a wide range of proteins, leading to significant changes in the size, zeta potential, and morphology of the graphene particle [74]. Using simulation-based (molecular dynamics) approaches, Chong and coworkers demonstrated that the adsorption of four highly abundant blood proteins onto GO and rGO was mainly enthalpically driven through strong π − π stacking interactions between the aromatic rings of the proteins and the graphene sp^2-carbons, although hydrophobic interactions also occurred [75]. However, basic residues such as arginine also play an equally important, or even more important, role during this process. The strong dispersion interactions between the side chains of these solvent-exposed basic residues and the graphene surface provide the driving force for a tight binding between these basic residues and graphene [76]. Graphene–protein interactions depend on the types of the proteins within the microenvironment. Ultimately, the decoration of the corona (i.e., the type, amount, and conformation of the attached proteins) can determine the biological fate of graphene [77]. On the other hand, Tenzer and coworkers show that various size and surface functionalization of nanoparticles could adsorb different profiles of human plasma coronas by assay of label-free snapshot proteomics [78]. Xu and coworkers prepared a series of GO derivatives, including aminated GO (GO-NH_2), poly(acrylamide)-functionalized GO (GO-PAM), poly(acrylic acid)-functionalized GO (GO-PAA), and poly(ethylene glycol)-functionalized GO (GO-PEG), and compared their toxicity with pristine GO. They hypothesized that

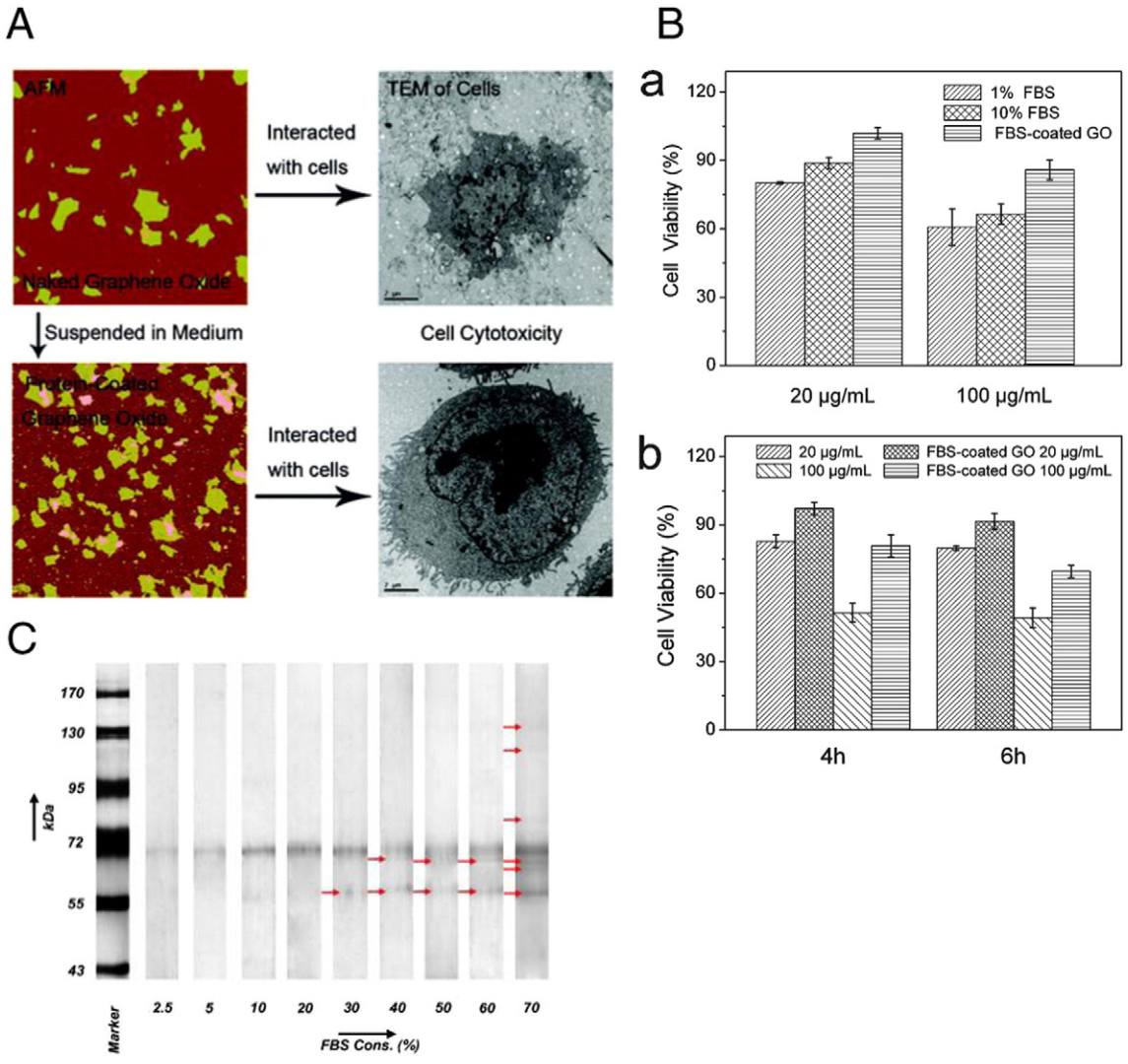

Fig. 7. Formation of the protein corona improves the biocompatibility. (A) Protein corona-mediated mitigation of cytotoxicity of graphene oxide. A549 cells were with GO nanosheets or FBS-coated GO nanosheets (100 μg/ml) at 37 °C for 2 h. The ultrastructure of cells were observed with TEM. GO exposure caused cell shrinkage and fragmentation in A549 cells, suggesting the induction of cell death. However, no apparent morphological alterations were observed in cells exposed to FBS-coated GO, indicating that protein corona mitigate the cytotoxicity of GO. (B) The quantification of FBS on cytotoxicity of GO nanosheets. (B-a) Cell viability of A549 cells treated with GO nanosheets (20 μg/ml, 100 μg/ml) dispersed in RPMI medium 1640 containing various concentrations of FBS for 2 h. (B-b) Cell viability of A549 cells treated with GO (10% FBS) and FBS-coated GO nanosheets for 4 and 6 h [80]. (C) SDS–PAGE analysis of hard corona human plasma proteins following incubation at different plasma concentrations [81]. Image adapted from References [80,81] with permission, copyright © American Chemical Society 2011 & Elsevier B.V. 2013.

the differences in biocompatibility might be due to the differential compositions of protein corona, especially immunoglobulin G (IgG). They deciphered the different components in protein corona, which determined the adsorption onto membrane and cellular uptake. It could be discerned that the profiles for each GO material were quite different, indicating the protein corona on various GO sheets was distinct, presumably due to their different size, surface charge (reflected by their zeta potential values), and hydrophobicity [49].

5.1.2. Formation of the protein corona improves the hemocompatibility

Nano-sized GO induces severe hemolysis in vitro; however, a proper surface coating can remarkably improve its hemocompatibility [79,80]. Hu and coworkers investigated the interactions between GO and serum proteins systematically. They found that upon serum exposure, the thickness of GO substantially increased to the range 4.0–18.0 nm from a thickness of 1.0 nm, suggesting that a large amount of proteins had coated the surfaces of the GO nanosheets (designated as FBS-coated GO). More importantly, they found that the formation of the serum albumin-based protein corona could mitigate the cytotoxicity of GO nanosheets. This may be due to the prevention of GO-induced physical damage to the cell membrane (Fig. 7A, B) [80]. Mao and coworkers compared the composition of protein coronas and found that by increasing the human plasma concentration, the affinity of low-molecular-weight proteins to the surfaces of graphene sheets is significantly increased (Fig. 7C) [81].

Cheng and coworkers reported that reduced graphene oxide (rGO) with corona composed with biopolymer functionalization have markedly elevated biocompatibility, which exhibit an ultra-low hemolysis ratio (lower than 1.8%) in human blood cells and has good cytocompatibility for human umbilical vein endothelial cells (HUVEC) even at a high concentration of 100 μg/ml [82]. Similar results have been obtained from other graphene derivatives. Papi and coworkers reported recently that after interacting with plasma proteins, nano-sized GO flakes, which can disrupt the erythrocyte plasma membrane, had greatly reduced hemolytic activities [83]. Mbeh and coworkers also reported that the preincubation of graphene-oxide nanoribbon (GONR; a relatively homogenous graphene-related nanomaterial synthesized using oxidative unzipping of multi-walled carbon nanotubes) with human plasma serum (HPS), leading to the formation of a protein corona on the surface of the GO nanoribbons, decreased the cytotoxicity markedly in HUVEC

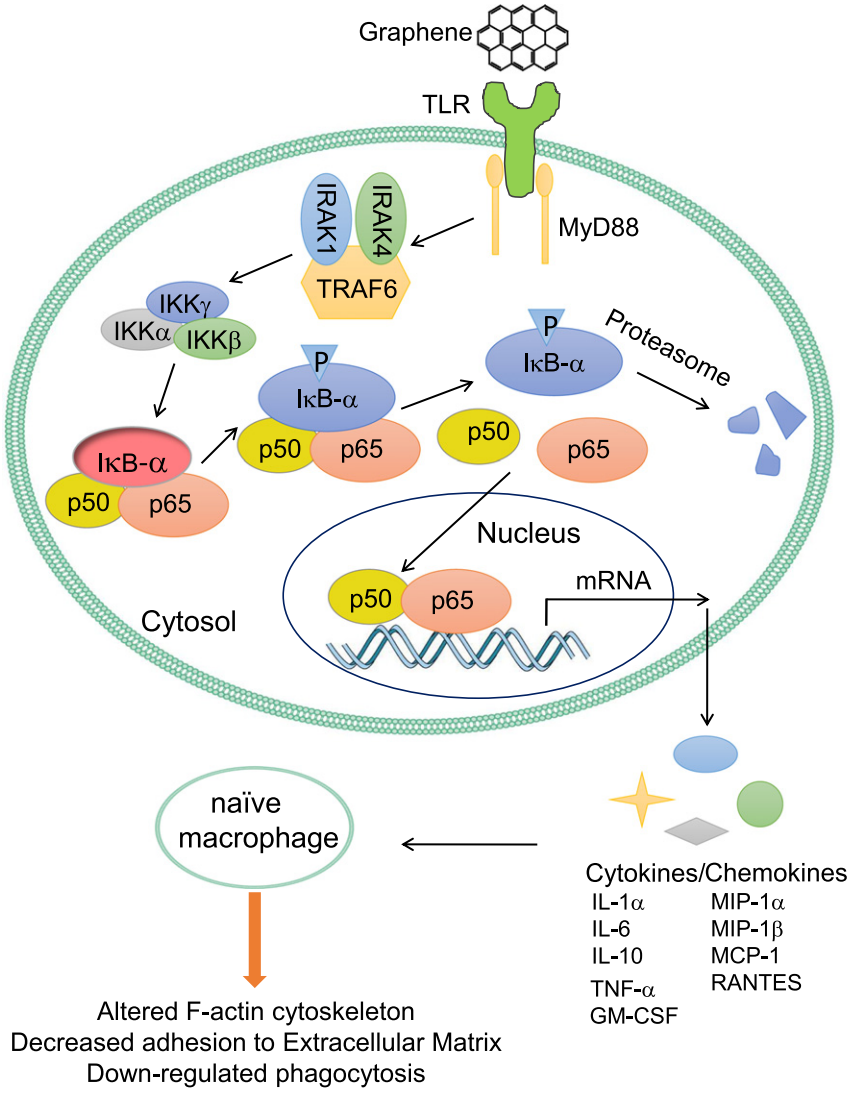

Fig. 8. Signaling pathway of macrophage activation stimulated by graphene nanosheets. Graphene may be recognized by certain types of TLRs, thus activating kinase cascades via a MyD88-dependent mechanism. Activation of IKK initiates the phosphorylation and consequent degradation of IκB, resulting in the release of NF-κB subunits, and their translocation into the nucleus. NF-κB binds to the promoter regions of its effector genes and initiates the transcription of multiple proinflammatory genes and the secretion of various proinflammatory factors, including IL-1α, IL-6, IL-10, TNF-α, CM-CSF, MCP-1, MIP-1α, MIP-1β, and RANTES. These proinflammatory factors modulate the immune responses of neighboring macrophages. Image adapted from Reference [89] with permission, copyright © Elsevier B.V. 2012.

cells [84]. The results mentioned above indicate that the interaction between graphene and biomolecules may provide an alternative and convenient route to enhancing the biocompatibility of graphene/biomolecule complexes through functional modification; these complexes could then be used for safe biomedical applications.

5.1.3. Potential medical applications based on graphene–protein interactions

Hajipour and coworkers developed "personalized protein coronas" by decorating GO sheets with plasma from human subjects with different diseases/conditions, including hypofibrinogenemia, leukemia, thalassemia, rheumatism, fauvism, hypercholesterolemia, diabetes, and pregnancy. These "personalized protein coronas" triggered different biological responses and exhibited significantly different properties in terms of cellular toxicity, apoptosis, cellular uptake, reactive oxygen species production, lipid peroxidation, and nitrogen oxide levels, which could help researchers to design efficient, safe, and patient-specific nanobiomaterials in a disease type-specific manner for clinical and biological applications [85]. The interaction between graphene and proteins also influences the biological functions of the proteins. Yang and coworkers reported that graphene can destroy amyloid fibrils through the penetration and extraction of peptides, which may be of potential use in the therapy of Alzheimer's disease [86].

5.2. Biological effects on macrophages

Recently, an increasing number of studies have focused on the interactions between graphene and immune cells; the majority of these works have been carried out in macrophages [87]. Macrophages, which differentiate from circulating monocytes, are key innate immune effector cells best known for their role as professional phagocytes. Macrophages have proteolytic and catabolic activities and ingest pathogens through phagocytosis, by scavenging cellular and exogenous debris, and by remodeling tissues after injury. These cells are also pivotal in the uptake of nanoparticles. Intravenously injected graphene-based nanomaterials are likely to be cleared out by macrophages before reaching their target sites. Graphene derivatives stimulate the activation of macrophages, thereby triggering the production and release of cytokines/chemokines that mediate the inflammatory responses.

5.2.1. Uptake of graphene by macrophages

Unlike non-phagocytic cells, macrophages uptake graphene effectively via phagocytosis that has already been explored. Yue and coworkers investigated the uptake of 2 μm and 350 nm GO particles in three cancer cell lines, and HUVEC endothelial cells, finding that the GO internalization was negligible in all of these non-phagocytes [88]. They suggested this might be due to strong electrostatic repulsions between GO particles and the negatively charged cell surface. In contrast to the low GO signal found in non-phagocytic cells, obvious increases in GO florescence were detected in primary murine macrophages and J774A.1 macrophages, suggesting that macrophages are highly capable of GO uptake. Moreover, active phagocytosis may be powerful enough to overcome the electrostatic repulsion barrier that exists in the macrophage–GO interaction. These authors further analyzed the detailed internalization behavior of GO in primary macrophages by selective inhibition of certain phagocytosis receptors, finding a significant reduction in uptake after the Fcγ receptor was blocked with IgG antibody. This result revealed a key role for the FcγR-mediated phagocytic pathway in GO entry.

Zhou and coworkers investigated the interaction between pristine graphene and macrophages. By combining confocal microscopy and live cell imaging, they dissected the molecular mechanisms by which graphene is internalized. They found that the ability of primary macrophages to uptake graphene is abolished by knockout of the MyD88 adaptor protein, suggesting the essential role of toll-like receptors (TLR) in the phagocytosis of pristine graphene [89].

5.2.2. Initiation of proinflammatory signaling pathways

After its phagocytosis by macrophages, graphene may initiate a cascade of events leading to inflammatory responses, which are characterized by the production and secretion of proinflammatory cytokines and chemokines. Yue and coworkers compared the effects of 2 μm and 350 nm GO particles on the production of interleukin-6 (IL-6), IL-10, IL-12, tumor necrosis factor (TNF)-α (TNF-α), monocyte chemotactic protein-1 (MCP-1), and interferon-γ (IFN-γ) in macrophages and found

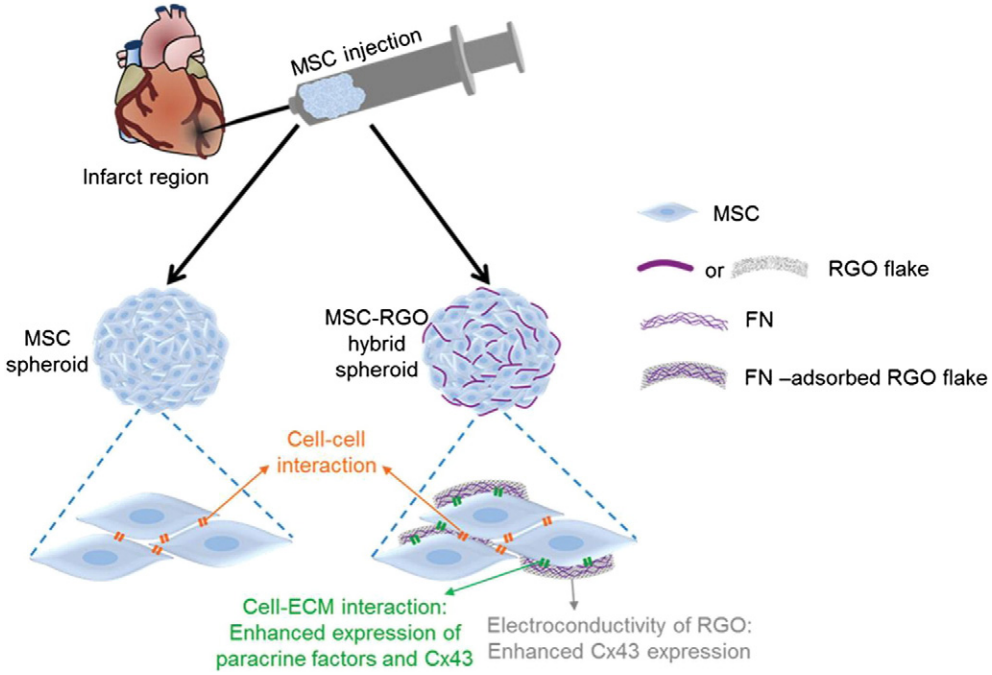

Fig. 9. Potential application of graphene in stem cell therapy. Reduced graphene oxide (rGO) shows high affinity toward extracellular matrix (ECM) proteins. By incorporating rGO flakes into mesenchymal stem cells (MSC) spheroids, it is possible to enhance the cell–ECM interactions and improve the therapeutic efficacy of MSCs for ischemic heart diseases. Image adapted from Reference [101] with permission, copyright © John Wiley & Sons Inc. 2015.

Table 1
Interactions between graphene-related nanomaterials and cells.

Material	Size	Functionalization	Cell types	Exposure conditions	Effects	References
Pristine graphene	Thickness: 2–3 nm; diameter: 172.7 ± 75.6 nm	–	Peritoneal macrophages; RAW264.7 cells	20 μg/mL for 24 h	The interaction of murine macrophages with pristine graphene results in elevated transcription and secretion of cytokines and chemokines, which is triggered by activation of the NF-κB signaling pathway	[89]
Pristine graphene	Thickness: 2–3 nm; size: 500–1000 nm	–	RAW 264.7	0–80 μg/mL for 24 or 48 h	Induction of cytotoxicity through the depletion of the mitochondrial membrane potential and the increase of intracellular reactive oxygen species, then trigger apoptosis by activation of the mitochondrial pathway.	[58]
Pristine graphene; functionalized graphene	Thickness: ~0.4 nm	Carboxylated	RAW 264.7	75 μg/mL for 24 h or 48 h	Macrophages showed relatively high intracellular uptake of functionalized, hydrophilic graphene compared to the hydrophobic pristine graphene.	[94]
Graphene; few layer graphene (FLG) microsheets	Lateral dimension: 0.5–10 μm; layer numbers: 4–25	–	Primary human keratinocytes; Human lung epithelial cells; Murine macrophages	5 h (macrophages)24 h (other cell types);	Graphene-related nanomaterials enter cells through spontaneous membrane penetration at edge asperities and corner sites	[44]
Graphene	Average grain size: ~10 μm	–	HeLa; Panc-1	–	The cellular responses to the graphene sheets are strongly dependent to either cell type or hard corona composition.	[81]
Graphene quantum dots (GQDs)	1.5–5.5 nm	–	THP-1	0–200 μg/mL, for 24, 48 or 72 h	GQDs induce inflammatory response, apoptosis, and autophagy in macrophages via p38 MAPK and NF-κB signaling pathways.	[60]
Pluronic dispersed graphene; GO	–	–	Lung cells	administered directly into the lungs of mice	Graphene-related nanomaterials increased the rate of mitochondrial respiration and the generation of reactive oxygen species, activating inflammatory and apoptotic pathways	[63]
Graphene, GO	Thickness: 3–4 nm; diameter: 100–200 nm	–	MDA-MB-231; B16F10; PC3	20 μg/ml; 24 h	Graphene or GO inhibits the migration and invasion of various cancer cells by inhibiting the activities of ETC complexes	[56]
Carboxyl graphene nanoplatelets (CXYG)	–	–	HepG2	0–32 μg/mL for 72 h	CXYG nanoplatelets caused cytotoxicity in HepG2 cells with plasma membrane damage and induction of oxidative stress	[48]
GO	Thickness: 6 nm; lateral size: 40 nm	–	HepG2	1–200 mg/L for 24 h	NADPH oxidase dependent ROS formation; deregulation of antioxidant/DNA repair/apoptosis related genes	[32]
GO	Thickness: ~1.0 nm; average size: 51 nm	–	GLC-82	100 mg/L for 48 h	Alters the miRNA expression profile	[34]
GO	385 nm	–	HepG2	0–16 μg/mL for 72 h	GO caused cytotoxicity in Hep G2 cells with plasma membrane damage and induction of oxidative stress	[48]
GO	Thickness: ~1.8 nm; size: 10–120 nm	PEG	RAW-264.7; Saos-2; 3T3	–	Impact on cytoskeleton; alterations in cell cycle	[50]
GO and its nanoassemblies	Size: 100–200 nm; thickness: 5–10 nm	layer-by-layer (LbL) assembly	Mouse embryonic fibroblast (MEF)	l μg/mL; 24–72 h	Without induction of noticeable harmful effects	[53]
GO, bGO, pGO-5, pGO-30, and GS	Hydrodynamic diameter in PBS: GO: 1678 ± 190 nm; bGO: 1574 ± 160 nm; pGO-5: 1254 ± 143 nm; pGO-30: 861 ± 115 nm; GS: 4312 ± 206 nm	–	Red blood cells; Human skin fibroblasts	0–200 μg/mL, for 3 h or 24 h	All the GO and GS show dose-dependent hemolytic activity on RBCs. Sonicated (smaller) GO exhibited higher hemolytic activity than untreated (larger) GO. Compared to individually dispersed GO sheets having higher surface oxygen content, the aggregated GS showed lower hemolytic activity.	[45]
GO	Thickness: 1.2 nm; average size: 200–260 nm	–	MEF	50 μg/mL for 24 h	As the oxidation degree decreased, GO derivatives led to a higher degree of cytotoxicity and apoptosis.	[65]
GO	Thickness: ~1 nm; lateral length: 0.2–1 μm	–	Human fibroblast cell	0–100 μg/mL 0–5 days	GO could produce cytotoxicity in dose- and time-dependent means, and can enter into cytoplasm and nucleus, decreasing cell adhesion, inducing cell floating and apoptosis.	[69]
GO	Thickness of GO: 0.9 nm; thickness of GO with protein corona: 5–10 nm	protein corona	Red blood cells	–	GO flakes have a very strong hemolytic activity increasing with the GO flakes size reduction. This activity was almost absent when the plasma protein corona was absorbed on the GO flakes surfaces.	[83]
GO	Thickness of GO-FBS: 4.0–18.0 nm	10% FBS	A549	20–100 μg/mL for 0–12 h	The cytotoxicity of GO is largely attenuated when GO is incubated with FBS, which is due to the extremely high protein adsorption ability of GO.	[80]
GO	–	–	Peritoneal macrophage; J774A.1;	0–20 μg/mL	The GO in micro-size induced much stronger inflammation responses while nano-sized graphene sheet showed better biocompatibility	[88]

			LLC; MCF-7; HepG2; Human umbilical vein endothelial cells (HUVEC)			
GO	Large GO: 2.4 μm Small GO: 350 nm	–	RAW264.7	5–100 μg/mL for 24 h.	GO treatment provoked the toll-like receptor (TLR) signaling cascades and triggered ensuing cytokine responses	[90]
GO	Thickness: 1 nm size: 1–2 μm	aminated; carboxylated	J774A.1; RAW 264.7	20 μg/mL for 24 h	Interaction of GO with TLR4 results in activation of TLR4 signaling, which is the predominant molecular basis for GO-mediated macrophagic necrosis.	[91]
GO	Large: 1.32 μm small: 0.27 μm very small: 0.13 μm	–	Human monocyte derived macrophages; Peritoneal macrophages	1–100 μg/mL for 24 h	GO sheet size had a significant impact on different cellular parameters (i.e. cellular viability, ROS generation, and cellular activation). The more the lateral dimensions of GO were reduced, the higher were the cellular internalization	[93]
GO, PVP-GO	Thickness of GO: 1.7 nm thickness of PVP-GO: 2.5 nm	PVP	Dendritic cells	25–100 μg/mL for 48 h	PVP-modified GO has a low immunogenicity than unadorned GO	[95]
GO, TiO_2-GO	diameter: 300 nm	–	A549	100 and 300 μg/ml for 4 h	GO enter A549 cells and located in the cytoplasm and nucleus without causing any cell damage. The TiO_2-GO composite separated into GO and TiO_2 after TiO_2-GO composite entered A549 cells	[68]
GO, sGO	GO: 0.5–3 μm sGO: <15 nm	–	PC-12	12.5 μg/mL for 48 h.	Inhibit Aβ peptide monomer fibrillation and clear mature amyloid fibrils	[86]
GO Flake	thickness: ~1.5 nm size: 1–6 μm	–	Mesenchymal stem cells (MSC)	10 μg/mL	GO flakes effectively prevent a series of adverse cell-signaling cascades that result in the anoikis of MSCs in response to ROS	[102]
GO	GO: 80 nm PEG-GO: 100 nm	PEG; labeled with FITC	Saos-2; HepG2; RAW-264.7	37.5 μg/mL FITC-PEG-GOs for 2 h	Several processes are involved in FITC-PEG-GOs uptake, including micropinocytosis, microtubule-dependent mechanisms, clathrin-dependent mechanisms, and phagocytosis	[36]
GO	Thickness: 1.1 nm; diameter: 0.84 ± 0.41 μm,	FITC-BSA	C2C12	20–50 μg/mL for 30 min–14 h	Small nanosheets enter cells mainly through clathrin-mediated endocytosis, and the increase of graphene size enhances phagocytotic uptake of the nanosheets.	[37]
GO	thickness: 2–3 nm lateral length: 100–200 nm	PEG	MDA-MB-231; MDA-MB-436; SK-BR-3	40 or 80 μg/ml for 24 h	PEG-GO inhibited the migratory and invasive properties of human metastatic breast cancer cell lines by inhibiting ATP synthesis, leading to a disruption of F-actin cytoskeletal assembly	[33]
NGO	Size: 5–50 nm	PEG	HCT-116		No apparent toxicity as drug carrier	[79]
NGO	Thickness: 1.4 nm; diameter: 20–40 nm	PEG-Ce6 PEG-BPEI-Ce6	HeLa	–	No apparent toxicity as drug carrier	[57]
Oxidized graphene nanoribbons (O-GNR)	width: 125–220 nm; lengths: 500–2500 nm	PEG-DSPE	HeLa; NIH-3T3; SKBR3; MCF7	10–400 μg/mL for 12–48 h	O-GNR-PEG-DSPEs show a dose-dependent and time-dependent cytotoxic effects on the four cell lines.	[39]
O-GNR	–	PEG-DSPE	MCF7; A549; MRC5	50 μg/mL for 30 min	Significant O-GNR-PEG-DSPE uptake into cells with high EGFR expression.	[42]
O-GNR	Average widths: 100–300 nm length: 500–2500 nm	PEG-DSPE	U251; CG-4; MCF-7	–	No apparent toxicity as drug carrier	[43]
O-GNR	Thickness: ~1.0 nm widths: ~100 nm	albumin	A549	0–100 μg/mL for 24 h	The protein-functionalized GONRs with concentrations ≤50 μg/mL showed no significant cytotoxicity on the cells. However, the high concentration of 100 μg/mL exhibited significant cytotoxicity resulted in decrease of cell growth and induction of cell apoptosis.	[84]
O-GNR, GNO, and GONP	O-GNR: (w)x(l) 60–90 nm × 500–1500 nm GNO: (d) 50–300 nm GONP: (d) 20–40 nm	DSPE-PEG	MSC	0–300 μg/mL 24–72 h	GNOs, GONRs, and GONPs at concentrations of less than 50 μg/ml for 24 or 72 h could be considered potentially safe incubation conditions for ex vivo labeling for MSCs.	[41]
GO; rGO	GO, lateral dimension: 0.5–3 μm; rGO, lateral dimension: 0.5–3 μm	blood proteins (bovine fibrinogen, immunoglobulin, transferrin, and bovine serum albumin)	A549	200 μg/mL 24 h	Protein-coated graphene resulted in a markedly less cytotoxicity than uncoated graphene	[75]

(continued on next page)

Table 1 (*continued*)

Material	Size	Functionalization	Cell types	Exposure conditions	Effects	References
GO, rGO	Thickness of: ~1 nm; Size: 0.4–0.8 μm	–	HUVEC	10 μg/mL	GO is found to be more toxic than rGO of same size. GO and RGO induce significant increases in both intercellular ROS levels and mRNA levels of HO1 and TrxR. Moreover, a significant amount of DNA damage is observed in GO-treated cells, but not in RGO-treated cells. Oxidative stress-induced cytotoxicity reduces with a decreasing extent of oxygen functional group density on the rGO surface.	[67]
GO, rGO		–	A549; RAW 264.7	0.0125–12.5 μg/cm^2 for 5 days	Cells treated with lower concentrations of GO/rGO did not lead to increases in ROS production. Cellular internalization of GO was observed in phagoendosomes without signs of any intracellular damage.	[40]
rGO/HArGO	~100 nm	ICG-loaded	KB	20 μg/ml for 24 h	No significant cell death observed in the absence of NIR irradiation	[15]
rGO	~150 nm	PNT-anchored	Ramos; CCRF-CEM	–	No apparent toxicity as drug carrier	[23]
rGO	thickness: 7 nm lateral size: 40 nm	–	HepG2	1–200 mg/L for 24 h	hydrophobic rGO was found to mostly adsorbed at cell surface without internalization, ROS generation by physical interaction, poor gene regulation	[32]
rGO	–	biopolymer functionalized	Human blood cells; HUVEC	1–100 μg/mL 24 h	The biocompatible biopolymer functionalized RGO exhibited excellent biocompatibility	[82]
rGO, GONP, rGONP,	–	–	MSC	0.01–100 μg/mL for 24 h	The rGONPs exhibited a strong potential in destruction of the cells with the threshold concentration of 1.0 mg/mL, while the cytotoxicity of the rGO sheets appeared at high concentration of 100 mg/mL after 1 h. The results indicated that interaction of graphene derivatives with stem cells strongly depends on the lateral size of the sheets.	[51]
GO, rGO	Thickness: 1 nm; size: 0.4–0.8 μm;	–	HUVEC	1–10 μg/mL for 24 or 48 h	GO exhibits higher toxicity than rGO due to ROS generation. Small flake size graphene exhibit greater cytotoxicity compared to larger sheets due to intracellular accumulation of graphene.	[67]
GO, rGO	Size: 0.2–5 μm	–	Human platelets	0–20 μg/mL	GO can evoke strong aggregatory response in platelets comparable to that elicited by thrombin.	[72]
GO, rGO, G-NH_2	Size: 2 μm	Amine-modified	Red blood cells	2–10 μg/mL for 3 h	G-NH_2 is not endowed with thrombotoxic property.	[103]
GO, rGO	GO: 100 nm to 10 μm rGO: 100 nm to 1.5 μm	–	U87 U118	100 μg/mL	GO and rGO enter glioma cells and have different cytotoxicity. Both types of platelets reduced cell viability and proliferation with increasing doses, but rGO was more toxic than GO. Moreover, the level of apoptotic markers increased in rGO-treated tumors. rGO induces cell death mostly through apoptosis.	[104]
rGO	Size: 100 nm − 1.5 μm.	Arg, Pro	U87	50 μg/mL	Reduction in GBM tumor volume was observed. rGO + Arg shows anti-angiogenic and pro-apoptotic characteristics.	[105]

that the secretion of inflammatory cytokines was highly dependent on the GO dosage, particularly for the 2 μm GO particles [88]. Zhou and coworkers demonstrated the biological effects of sub-cytotoxic concentrations of pristine graphene on both primary murine macrophages and immortalized macrophages. They reported that graphene significantly stimulates the secretion of Th1/Th2 cytokines, including IL-1α, IL-6, IL-10, TNF-α, and granulocyte macrophage colony-stimulating factor (GM-CSF), as well as chemokines, including MCP-1, macrophage inflammatory protein-1α (MIP-1α), MIP-1β, and regulated on activation, normal T Cell expressed and secreted (RANTES), probably by activating TLR-mediated and NF-κB-dependent transcription (Fig. 8) [89]. Li and coworkers reported that pristine graphene activated both the MAPK and transforming growth factor-β (TGF-β)-related signaling pathways in macrophages [58]. Chen and coworkers reported that GO treatment of macrophages activated the TLR signaling cascades. TLR4 and TLR9 and their downstream signaling mediators MyD88, TRAF6, and NF-κB were also found to play pivotal roles in the GO-induced inflammatory responses [90].

5.2.3. Graphene-induced inflammation responses

The initiation of proinflammatory signaling and the production of proinflammatory cytokines and chemokines cause significant biological effects on both macrophages and neighboring cells. By using a coculture system, Zhou and coworkers exposed naïve macrophages to factors secreted by graphene-exposed macrophages, finding that the factors altered the morphology of naïve macrophages by remodeling their actin assembly, and, as a result, markedly decreased their ability to adhere to the extracellular matrix. The ability of these cells to undergo phagocytosis was also attenuated. Based on this evidence, these authors suggested that in graphene-exposed macrophages, the immune response underwent negative feedback. Moreover, they hypothesized that the graphene-induced factors may play an important role in the prevention of over-activation after graphene exposure [89]. However, when macrophages are exposed to high concentrations of graphene, they might undergo different types of cell death. Li and coworkers reported that pristine graphene activated Bim and Bax, two pro-apoptotic member of the Bcl-2 protein family, via the MAPK and TGF-β signaling pathways in macrophages. Consequently, caspase 3 and its downstream effector proteins, such as PARP, were activated, resulting in the execution of apoptosis [58]. Graphene also induced autophagy in macrophages [90]. Qu and coworkers demonstrated that GO induced necrotic cell death in macrophages, which is mediated by activation of TLR4 signaling and subsequently by TNF-α production [91].

5.2.4. Control of graphene-induced inflammation

Macrophage-initiated inflammation contributes to graphene-induced tissue damage in vivo. GO exposure has been shown to cause severe lung inflammation in mice, which is accompanied by bronchoalveolar lavage fluid pleocytosis, which consists of the leakage of protein into the alveolar space, and elevated levels of proinflammatory cytokines [63].

Graphene-induced inflammation responses could be regulated by different approaches, including controlling the size and thickness of the graphene sheet and surface modification. Bussy and coworkers considered the key physicochemical characteristics (the structure, surface, and colloidal properties) of graphene at the cellular, tissue, and whole body physiological levels, summarizing the evidence for health effects at all three levels. They offered a set of rules for the development of graphene and its derivatives to enhance the overall safety and minimize the risks for adverse reactions in humans due to graphene exposure. For instance, they recommended the use of small, individual graphene sheets that can be efficiently internalized by macrophages and removed from the site of deposition [92]. It should be noted that the GO sheet size has a significant impact on the different parameters of macrophages (i.e., cellular viability, cellular activation, and ROS generation) [93]. Compared with 2 μm-sized GO, 350 nm-sized GO only triggered moderate proinflammatory cytokine production in vitro and mediated slight inflammation cell infiltration in vivo [88].

Surface modification also influences the interaction between graphene and macrophages. Sasidharan and coworkers tested both pristine and functionalized graphene for their interactions with murine macrophages, finding that the toxicity of hydrophobic pristine samples could be significantly reduced by surface functionalization [94]. The enhanced biocompatibility of graphene by surface modification was also observed in other cell types of the immune system, including dendritic cells (DCs) and T lymphocytes [95].

The interaction of graphene with the immune system is still at a very early stage of investigation. This comprehensive investigation will provide a useful compass to guide future research in biomedicine. Understanding and controlling the interaction of graphene-based materials with macrophages is key to the development of graphene-enabled biomedical technologies and to the management of graphene health and safety issues [96].

5.3. Biological effects on cancer cells

Numerous nanomaterials such as liposomes, polymers/dendrimers, metal nanostructures, and carbon nanostructures are used to selectively target drugs to tumors. Among them, nanomaterials fabricated using graphene have drawn considerable attention for use in biomedical applications due to their unique physical and chemical properties. The large surface area of carbon-based nanomaterials has made them good drug carrier candidates. However, unmodified pristine graphene tends to form aggregates due to its hydrophobic nature, which limits its biomedical application. In 2008, Liu and coworkers overcame the aggregation issue of graphene by using a more hydrophilic derivative of graphene, PEGylated GO. They used the GO nanosheet for the intracellular delivery of water-insoluble anticancer agents and obtained significant tumor suppression effects in vitro and in vivo [79]. Since then, the application of GO as an effective drug nanocarrier has sparked growing interests in the biomedical field for cancer therapy [97]. Graphene derivatives could also be used as photothermal therapeutic agents [98] and imaging agents in cancer research due to their photo and thermal characteristics. For example, silver-embedded nanoparticles deposited onto doxorubicin-coupled GO exhibit very high drug-loading efficiency, impart excellent chemo-photothermal therapeutic efficacy, tumor targeting, and laser-controlled drug release, and aid in enhancing X-ray imaging [99].

Functionalized graphene can act as efficient anticancer nanoplatform [26], whereas graphene itself shows tumor suppression effects in vitro and in vivo. Zhou and coworkers reported that low concentrations of pristine graphene and GO show no apparent influence on the viability of MDA-MB-231 human breast cancer cells, PC3 human prostate cancer cells, or B16F10 mouse melanoma cells. However, both pristine graphene and GO can effectively inhibit the migration and invasion of these cancer cells in vitro [56] and in vivo [33]. An in situ analysis of cell metabolism indicated that both pristine graphene and GO decreased the electron transfer chain activity and caused a reduction in the production of ATP, which impaired the assembly of the actin cytoskeleton that is crucial for the migration and invasion of metastatic cancer cells [56].

Using systems biology-based approaches, Zhou and coworkers compared the differentially expressed proteins in cancer cells and non-cancerous epithelial cells exposed to GO. Interestingly, GO selectively targeted the key switch molecule of the cell metabolism, PGC-1α, in breast cancer cells, and down-regulated the expression of its effector genes, including the core subunits of the OXPHOS complex. Thus, GO was shown to remodel the metabolism of cancer cells [33].

5.4. Biological effects on stem cells

Based on their controllable biocompatibility, graphene and graphene-related nanomaterials could be used in tissue engineering, and thus the interaction between graphene and stem cells is an important research

area. Kim and coworkers summarized the potential of graphene or its derivatives for stem cell applications, with a particular focus on guiding stem cell differentiation, effective monitoring of their differentiation, stem cell delivery/transplantation, and promoting stem cell growth [100]. For example, MSC has emerged as a potential modality for myocardial infarction treatment through the secretion of paracrine factors and a gap junction protein to promotes cardiac repair and function restoration. Park and coworkers incorporates fibronectin-adsorbed rGO flakes into MSC spheroids, which enhances the cell-extracellular matrix (ECM) interactions, increases the paracrine factor expression, and up-regulates gap junction protein connexin 43. The injection of MSC-rGO hybrid spheroids into the infarcted hearts enhances cardiac repair compared with the injection of rGO flakes or MSC spheroids (Fig. 9) [101]. Park and coworkers also uses the GO flakes to protect the implanted MSCs from ROS-mediated death and thereby improve the therapeutic efficacy of the MSCs [102]. These effect likely due to the high affinity toward ECM proteins and the electrical conductivity of rGO and GO. These studies demonstrate that graphene can effectively improve the therapeutic efficacy, such as MSCs for ischemic heart diseases. Progression of effects on stem cells will promote and accelerate the use of graphene-based materials for stem cell-based approaches to cure various incurable diseases/disorders.

6. Conclusions, challenges, and future perspectives

Since its discovery in 2004, significant advances have been made in the development of graphene and graphene-related materials. They have exhibited a wide range of potential applications in different fields including electronics, energy engineering, and biomedicine. Recently, the number of biological studies involving graphene-related materials has rapidly increased, in which the effects of the biological interactions between graphene and living systems were documented. In the present review, we focuses on the molecular mechanisms underlying the interactions between graphene-related nanomaterials and cells and provides a systematic review of how graphene may interact with biomolecules, cross the plasma membrane, translocate within the endosome/lysosome systems, and affect key cellular components including mitochondrion, nucleus, and cytoskeleton (Table 1).

The interaction between graphene-related nanomaterials and plasma membrane and its transportation across the plasma membrane are key steps involved in the induction of biological effects, which are closely related with the physicochemical properties of graphene, including size, shape, and surface chemistry. By manipulating these properties, we can enhance the transportation efficacy of graphene-related materials, and diminish their side-effects. For example, small-sized (nano-sized) graphene derivatives with moderate oxidation status are generally more prone to be internalized into cells via endocytosis; based on these intrinsic properties, nano-sized GO derivatives could be used as efficient drug or gene carriers. The cytotoxicity effects of graphene-related materials could also be mitigated by surface modification with biocompatible molecules (e.g. natural proteins, peptides, and sugars).

This review also provided important information about the interactions between graphene-related nanomaterials and their effector cells, including immune cells, cancer cells, and stem cells. After their administration into the body, graphene-related materials cause a complicated impact on the immune system. On one hand, graphene could activate the macrophages and thus induce an immunoactivation response; on the other hand, high concentration of graphene could also induce apoptosis in macrophages and induce an immunosuppression response. Physicochemical properties of graphene-related materials, including size, shape, and surface chemistry, determine the immune responses; accordingly, graphene-related materials may act as immunotherapy tools after a suitable surface modification.

Cancer therapy is one of the hottest topics in the biomedical application of graphene-related nanomaterials. Due to their small size, large surface area, and versatile chemistry, graphene-related materials are regarded as ideal building blocks for drug carrier, which tend to selectively accumulate in tumor tissue owing to the enhanced permeability and retention effect. Information about the interactions between graphene and cancer cells provides new strategies for selective targeting graphene to cancer cells. For example, cancer cell-specific uptake of graphene could be further improved by modification with various targeting molecules, include folic acid, antibodies, DNA aptamers, transferrin, and peptides. By integrating chemotherapy agents, photothermal therapy agents, and multimodal imaging probes on the graphene core, multifunctional nanoplatforms for cancer theragnosis have been successfully developed.

Based on the information about the interactions between graphene and stem cells, a series of engineered graphene-related nanomaterials with improved high biocompatibility have been developed, which show promising potential in the fields of tissue engineering and regenerative medicine. Proper surface engineering endow graphene with a strong adsorbing capacity for both small molecules and biomacromolecules, which are essential for the growth and differentiation of stem cells.

Although the toxicity of graphene-related materials in vitro and in vivo could be mitigated by controlling the size, shape, and surface chemistry, the long-term toxicity is still a crucial issue. However, knowledge about the biodegradation and metabolism of graphene-related materials is still limited. The design and development of biodegradable graphene derivatives through optimizing the physicochemical properties and structural modification is an important step to obtain graphene-related materials with excellent biocompatibility and biosafety, which will satisfy the clinical requirements in nanomedicine in the future.

Acknowledgments

This work was supported by grant from the National Basic Research Program of China (grant no. 2012CB934003), the Major Equipment Program of China (grant no. 2011YQ030134), and the National Natural Science Foundation of China (grant nos. 31470814 and 31300683).

References

[1] K.S. Novoselov, A.K. Geim, S.V. Morozov, D. Jiang, Y. Zhang, S.V. Dubonos, I.V. Grigorieva, A.A. Firsov, Electric field effect in atomically thin carbon films, Science 306 (2004) 666–669.
[2] A.K. Geim, K.S. Novoselov, The rise of graphene, Nat. Mater. 6 (2007) 183–191.
[3] W. Han, R.K. Kawakami, M. Gmitra, J. Fabian, Graphene spintronics, Nat. Nanotechnol. 9 (2014) 794–807.
[4] C.L. Tan, Z.D. Liu, W. Huang, H. Zhang, Non-volatile resistive memory devices based on solution-processed ultrathin two-dimensional nanomaterials, Chem. Soc. Rev. 44 (2015) 2615–2628.
[5] X.Q. Xie, K. Kretschmer, G.X. Wang, Advances in graphene-based semiconductor photocatalysts for solar energy conversion: fundamentals and materials engineering, Nanoscale 7 (2015) 13278–13292.
[6] Q.J. Xiang, B. Cheng, J.G. Yu, Graphene-based photocatalysts for solar-fuel generation, Angew. Chem. Int. Ed. 54 (2015) 11350–11366.
[7] M. Srivastava, J. Singh, T. Kuila, R.K. Layek, N.H. Kim, J.H. Lee, Recent advances in graphene and its metal-oxide hybrid nanostructures for lithium-ion batteries, Nanoscale 7 (2015) 4820–4868.
[8] X.B. Fan, G.L. Zhang, F.B. Zhang, Multiple roles of graphene in heterogeneous catalysis, Chem. Soc. Rev. 44 (2015) 3023–3035.
[9] I.V. Pavlidis, M. Patila, U.T. Bornscheuer, D. Gournis, H. Stamatis, Graphene-based nanobiocatalytic systems: recent advances and future prospects, Trends Biotechnol. 32 (2014) 312–320.
[10] F. Perreault, A.F. de Faria, M. Elimelech, Environmental applications of graphene-based nanomaterials, Chem. Soc. Rev. 44 (2015) 5861–5896.
[11] J.M. Yoo, J.H. Kang, B.H. Hong, Graphene-based nanomaterials for versatile imaging studies, Chem. Soc. Rev. 44 (2015) 4835–4852.
[12] J. Bartelmess, S.J. Quinn, S. Giordani, Carbon nanomaterials: multi-functional agents for biomedical fluorescence and Raman imaging, Chem. Soc. Rev. 44 (2015) 4672–4698.
[13] M. Orecchioni, R. Cabizza, A. Bianco, L.G. Delogu, Graphene as cancer theranostic tool: progress and future challenges, Theranostics 5 (2015) 710–723.
[14] D.Q. Chen, C.A. Dougherty, K.C. Zhu, H. Hong, Theranostic applications of carbon nanomaterials in cancer: focus on imaging and cargo delivery, J. Control. Release 210 (2015) 230–245.
[15] W. Miao, G. Shim, G. Kim, S. Lee, H.J. Lee, Y.B. Kim, Y. Byun, Y.K. Oh, Image-guided synergistic photothermal therapy using photoresponsive imaging agent-loaded graphene-based nanosheets, J. Control. Release 211 (2015) 28–36.
[16] M.S. Draz, B.A. Fang, P.F. Zhang, Z. Hu, S.D. Gu, K.C. Weng, J.W. Gray, F.F. Chen, Nanoparticle-mediated systemic delivery of siRNA for treatment of cancers and viral infections, Theranostics 4 (2014) 872–892.

[17] X.L. Ding, H.F. Liu, Y.B. Fan, Graphene-based materials in regenerative medicine, Adv. Healthcare Mater. 4 (2015) 1451–1468.
[18] F. Menaa, A. Abdelghani, B. Menaa, Graphene nanomaterials as biocompatible and conductive scaffolds for stem cells: impact for tissue engineering and regenerative medicine, J. Tissue Eng. Regen. Med. 9 (2015) 1321–1338.
[19] Z.Y. Wang, Z.H. Dai, Carbon nanomaterial-based electrochemical biosensors: an overview, Nanoscale 7 (2015) 6420–6431.
[20] S.J. Heerema, C. Dekker, Graphene nanodevices for DNA sequencing, Nat. Nanotechnol. 11 (2016) 127–136.
[21] K. Yang, L.Z. Feng, Z. Liu, The advancing uses of nano-graphene in drug delivery, Expert Opin. Drug Del. 12 (2015) 601–612.
[22] K. Muthoosamy, R.G. Bai, S. Manickam, Graphene and graphene oxide as a docking station for modern drug delivery system, Curr. Drug Deliv. 11 (2014) 701–718.
[23] M.G. Kim, J.Y. Park, W. Miao, J. Lee, Y.K. Oh, Polyaptamer DNA nanothread-anchored, reduced graphene oxide nanosheets for targeted delivery, Biomaterials 48 (2015) 129–136.
[24] Y.Q. Yang, A.M. Asiri, Z.W. Tang, D. Du, Y.H. Lin, Graphene based materials for biomedical applications, Mater. Today 16 (2013) 365–373.
[25] F.M. Tonelli, V.A. Goulart, K.N. Gomes, M.S. Ladeira, A.K. Santos, E. Lorencon, L.O. Ladeira, R.R. Resende, Graphene-based nanomaterials: biological and medical applications and toxicity, Nanomedicine (London) 10 (2015) 2423–2450.
[26] S.C. Patel, S. Lee, G. Lalwani, C. Suhrland, S.M. Chowdhury, B. Sitharaman, Graphene-based platforms for cancer therapeutics, Ther. Deliv. 7 (2016) 101–116.
[27] K. Yang, L. Feng, Z. Liu, Stimuli responsive drug delivery systems based on nano-graphene for cancer therapy, Adv. Drug Deliv. Rev. 105 (2016) 228–241.
[28] J. Lin, X. Chen, P. Huang, Graphene-based nanomaterials for bioimaging, Adv. Drug Deliv. Rev. 105 (2016) 242–254.
[29] Y.W. Chen, Y.L. Su, S.H. Hu, S.Y. Chen, Functionizalized Graphene Nanocomposites for Enhancing Photothermal Therapy in Tumor Treatment, Adv. Drug Deliv. Rev. 105 (2016) 190–204.
[30] S.F. Kiew, L.V. Kiew, H.B. Lee, T. Imae, L.Y. Chung, Assessing biocompatibility of graphene oxide-based nanocarriers: a review, J. Control. Release 226 (2016) 217–228.
[31] G. Lalwani, M. D'Agati, A.M. Khan, B. Sitharaman, Toxicology of graphene-based nanomaterials, Adv. Drug Deliv. Rev. 105 (2016) 109–144.
[32] N. Chatterjee, H.J. Eom, J. Choi, A systems toxicology approach to the surface functionality control of graphene–cell interactions, Biomaterials 35 (2014) 1109–1127.
[33] T. Zhou, B. Zhang, P. Wei, Y. Du, H. Zhou, M. Yu, L. Yan, W. Zhang, G. Nie, C. Chen, Y. Tu, T. Wei, Energy metabolism analysis reveals the mechanism of inhibition of breast cancer cell metastasis by PEG-modified graphene oxide nanosheets, Biomaterials 35 (2014) 9833–9843.
[34] Y.P. Li, Q.L. Wu, Y.L. Zhao, Y.F. Bai, P.S. Chen, T. Xia, D.Y. Wang, Response of microRNAs to in vitro treatment with graphene oxide, ACS Nano 8 (2014) 2100–2110.
[35] J. Mao, R. Guo, L.T. Yan, Simulation and analysis of cellular internalization pathways and membrane perturbation for graphene nanosheets, Biomaterials 35 (2014) 6069–6077.
[36] J. Linares, M.C. Matesanz, M. Vila, M.J. Feito, G. Goncalves, M. Vallet-Regi, P.A. Marques, M.T. Portoles, Endocytic mechanisms of graphene oxide nanosheets in osteoblasts, hepatocytes and macrophages, ACS Appl. Mater. Interfaces 6 (2014) 13697–13706.
[37] Q. Mu, G. Su, L. Li, B.O. Gilbertson, L.H. Yu, Q. Zhang, Y.P. Sun, B. Yan, Size-dependent cell uptake of protein-coated graphene oxide nanosheets, ACS Appl. Mater. Interfaces 4 (2012) 2259–2266.
[38] S.E. Gratton, P.A. Ropp, P.D. Pohlhaus, J.C. Luft, V.J. Madden, M.E. Napier, J.M. DeSimone, The effect of particle design on cellular internalization pathways, Proc. Natl. Acad. Sci. U. S. A. 105 (2008) 11613–11618.
[39] S. Mullick Chowdhury, G. Lalwani, K. Zhang, J.Y. Yang, K. Neville, B. Sitharaman, Cell specific cytotoxicity and uptake of graphene nanoribbons, Biomaterials 34 (2013) 283–293.
[40] L. Horvath, A. Magrez, M. Burghard, K. Kern, L. Forro, B. Schwaller, Evaluation of the toxicity of graphene derivatives on cells of the lung luminal surface, Carbon 64 (2013) 45–60.
[41] Y. Talukdar, J.T. Rashkow, G. Lalwani, S. Kanakia, B. Sitharaman, The effects of graphene nanostructures on mesenchymal stem cells, Biomaterials 35 (2014) 4863–4877.
[42] S. Mullick Chowdhury, P. Manepalli, B. Sitharaman, Graphene nanoribbons elicit cell specific uptake and delivery via activation of epidermal growth factor receptor enhanced by human papillomavirus E5 protein, Acta Biomater. 10 (2014) 4494–4504.
[43] S.M. Chowdhury, C. Surhland, Z. Sanchez, P. Chaudhary, M.A.S. Kumar, S. Lee, L.A. Pena, M. Waring, B. Sitharaman, M. Naidu, Graphene nanoribbons as a drug delivery agent for lucanthone mediated therapy of glioblastoma multiforme, Nanomed. Nanotechnol. 11 (2015) 109–118.
[44] Y.F. Li, H.Y. Yuan, A. von dem Bussche, M. Creighton, R.H. Hurt, A.B. Kane, H.J. Gao, Graphene microsheets enter cells through spontaneous membrane penetration at edge asperities and corner sites, Proc. Natl. Acad. Sci. U. S. A. 110 (2013) 12295–12300.
[45] K.H. Liao, Y.S. Lin, C.W. Macosko, C.L. Haynes, Cytotoxicity of graphene oxide and graphene in human erythrocytes and skin fibroblasts, ACS Appl. Mater. Interfaces 3 (2011) 2607–2615.
[46] L.M. Saeed, M. Mahmood, S.J. Pyrek, T. Fahmi, Y. Xu, T. Mustafa, Z.A. Nima, S.M. Bratton, D. Casciano, E. Dervishi, A. Radominska-Pandya, A.S. Biris, Single-walled carbon nanotube and graphene nanodelivery of gambogic acid increases its cytotoxicity in breast and pancreatic cancer cells, J. Appl. Toxicol. 34 (2014) 1188–1199.
[47] J. Wu, R. Yang, L. Zhang, Z. Fan, S. Liu, Cytotoxicity effect of graphene oxide on human MDA-MB-231 cells, Toxicol. Mech. Methods 25 (2015) 312–319.
[48] T. Lammel, P. Boisseaux, M.L. Fernandez-Cruz, J.M. Navas, Internalization and cytotoxicity of graphene oxide and carboxyl graphene nanoplatelets in the human hepatocellular carcinoma cell line Hep G2, Part. Fibre. Toxicol. 10 (2013) 27.
[49] M. Xu, J.Q. Zhu, F.F. Wang, Y.J. Xiong, Y.K. Wu, Q.Q. Wang, J. Weng, Z.H. Zhang, W. Chen, S.J. Liu, Improved in vitro and in vivo biocompatibility of graphene oxide through surface modification: poly(acrylic acid)-functionalization is superior to PEGylation, ACS Nano 10 (2016) 3267–3281.
[50] M.C. Matesanz, M. Vila, M.J. Feito, J. Linares, G. Goncalves, M. Vallet-Regi, P.A. Marques, M.T. Portoles, The effects of graphene oxide nanosheets localized on F-actin filaments on cell-cycle alterations, Biomaterials 34 (2013) 1562–1569.
[51] O. Akhavan, E. Ghaderi, A. Akhavan, Size-dependent genotoxicity of graphene nanoplatelets in human stem cells, Biomaterials 33 (2012) 8017–8025.
[52] E.L.K. Chng, C.K. Chua, M. Pumera, Graphene oxide nanoribbons exhibit significantly greater toxicity than graphene oxide nanoplatelets, Nanoscale 6 (2014) 10792–10797.
[53] Y.Y. Li, Z.Z. Lu, Z.J. Li, G.J. Nie, Y. Fang, Cellular uptake and distribution of graphene oxide coated with layer-by-layer assembled polyelectrolytes, J. Nanopart. Res. 16 (2014).
[54] J.Q. Chen, H.Y. Liu, C.B. Zhao, G.Q. Qin, G.N. Xi, T. Li, X.P. Wang, T.S. Chen, One-step reduction and PEGylation of graphene oxide for photothermally controlled drug delivery, Biomaterials 35 (2014) 4986–4995.
[55] J. Kim, L.J. Cote, F. Kim, J. Huang, Visualizing graphene based sheets by fluorescence quenching microscopy, J. Am. Chem. Soc. 132 (2010) 260–267.
[56] H. Zhou, B. Zhang, J. Zheng, M. Yu, T. Zhou, K. Zhao, Y. Jia, X. Gao, C. Chen, T. Wei, The inhibition of migration and invasion of cancer cells by graphene via the impairment of mitochondrial respiration, Biomaterials 35 (2014) 1597–1607.
[57] Y.P. Zeng, Z.Y. Yang, S.L. Luo, H. Li, C. Liu, Y.H. Hao, J. Liu, W.D. Wang, R. Li, Fast and facile preparation of PEGylated graphene from graphene oxide by lysosome targeting delivery of photosensitizer to efficiently enhance photodynamic therapy, RSC Adv. 5 (2015) 57725–57734.
[58] Y. Li, Y. Liu, Y.J. Fu, T.T. Wei, L. Le Guyader, G. Gao, R.S. Liu, Y.Z. Chang, C.Y. Chen, The triggering of apoptosis in macrophages by pristine graphene through the MAPK and TGF-beta signaling pathways, Biomaterials 33 (2012) 402–411.
[59] B. Wan, Z.X. Wang, Q.Y. Lv, P.X. Dong, L.X. Zhao, Y. Yang, L.H. Guo, Single-walled carbon nanotubes and graphene oxides induce autophagosome accumulation and lysosome impairment in primarily cultured murine peritoneal macrophages, Toxicol. Lett. 221 (2013) 118–127.
[60] Y. Qin, Z.W. Zhou, S.T. Pan, Z.X. He, X. Zhang, J.X. Qiu, W. Duan, T. Yang, S.F. Zhou, Graphene quantum dots induce apoptosis, autophagy, and inflammatory response via p38 mitogen-activated protein kinase and nuclear factor-kappaB mediated signaling pathways in activated THP-1 macrophages, Toxicology 327 (2015) 62–76.
[61] X. Hu, S. Ouyang, L. Mu, J. An, Q. Zhou, Effects of graphene oxide and oxidized carbon nanotubes on the cellular division, microstructure, uptake, oxidative stress, and metabolic profiles, Environ. Sci. Technol. 49 (2015) 10825–10833.
[62] A. Jarosz, M. Skoda, I. Dudek, D. Szukiewicz, Oxidative stress and mitochondrial activation as the main mechanisms underlying graphene toxicity against human cancer cells, Oxid. Med. Cell. Longev. (2016), http://dx.doi.org/10.1155/2016/5851035.
[63] M.C. Duch, G.R.S. Budinger, Y.T. Liang, S. Soberanes, D. Urich, S.E. Chiarella, L.A. Campochiaro, A. Gonzalez, N.S. Chandel, M.C. Hersam, G.M. Mutlu, Minimizing oxidation and stable nanoscale dispersion improves the biocompatibility of graphene in the lung, Nano Lett. 11 (2011) 5201–5207.
[64] W. Zhang, C. Wang, Z. Li, Z. Lu, Y. Li, J.J. Yin, Y.T. Zhou, X. Gao, Y. Fang, G. Nie, Y. Zhao, Unraveling stress-induced toxicity properties of graphene oxide and the underlying mechanism, Adv. Mater. 24 (2012) 5391–5397.
[65] W. Zhang, L. Yan, M. Li, R. Zhao, X. Yang, T. Ji, Z. Gu, J.J. Yin, X. Gao, G. Nie, Deciphering the underlying mechanisms of oxidation-state dependent cytotoxicity of graphene oxide on mammalian cells, Toxicol. Lett. 237 (2015) 61–71.
[66] C.Y. Wu, C. Wang, T. Han, X.J. Zhou, S.W. Guo, J.Y. Zhang, Insight into the cellular internalization and cytotoxicity of graphene quantum dots, Adv. Healthcare Mater. 2 (2013) 1613–1619.
[67] S. Das, S. Singh, V. Singh, D. Joung, J.M. Dowding, D. Reid, J. Anderson, L. Zhai, S.I. Khondaker, W.T. Self, S. Seal, Oxygenated functional group density on graphene oxide: its effect on cell toxicity, Part. Part. Syst. Charact. 30 (2013) 148–157.
[68] C. Jin, F.D. Wang, Y. Tang, X.Z. Zhang, J.Q. Wang, Y.J. Yang, Distribution of graphene oxide and TiO2-graphene oxide composite in A549 cells, Biol. Trace Elem. Res. 159 (2014) 393–398.
[69] K. Wang, J. Ruan, H. Song, J.L. Zhang, Y. Wo, S.W. Guo, D.X. Cui, Biocompatibility of graphene oxide, Nanoscale Res. Lett. 6 (2011).
[70] C. Wang, C.Y. Wu, X.J. Zhou, T. Han, X.Z. Xin, J.Y. Wu, J.Y. Zhang, S.W. Guo, Enhancing cell nucleus accumulation and DNA cleavage activity of anti-cancer drug via graphene quantum dots, Sci. Rep-Uk 3 (2013).
[71] G.Y. Chen, C.L. Meng, K.C. Lin, H.Y. Tuan, H.J. Yang, C.L. Chen, K.C. Li, C.S. Chiang, Y.C. Hu, Graphene oxide as a chemosensitizer: diverted autophagic flux, enhanced nuclear import, elevated necrosis and improved antitumor effects, Biomaterials 40 (2015) 12–22.
[72] S.K. Singh, M.K. Singh, M.K. Nayak, S. Kumari, S. Shrivastava, J.J. Gracio, D. Dash, Thrombus inducing property of atomically thin graphene oxide sheets, ACS Nano 5 (2011) 4987–4996.
[73] N. Duran, D.S. Martinez, C.P. Silveira, M. Duran, A.C. de Moraes, M.B. Simoes, O.L. Alves, W.J. Favaro, Graphene oxide: a carrier for pharmaceuticals and a scaffold for cell interactions, Curr. Top. Med. Chem. 15 (2015) 309–327.
[74] X.Q. Wei, L.Y. Hao, X.R. Shao, Q. Zhang, X.Q. Jia, Z.R. Zhang, Y.F. Lin, Q. Peng, Insight into the interaction of graphene oxide with serum proteins and the impact of the degree of reduction and concentration, ACS Appl. Mater. Interfaces 7 (2015) 13367–13374.
[75] Y. Chong, C. Ge, Z. Yang, J.A. Garate, Z. Gu, J.K. Weber, J. Liu, R. Zhou, Reduced cytotoxicity of graphene nanosheets mediated by blood-protein coating, ACS Nano 9 (2015) 5713–5724.
[76] Z. Gu, Z. Yang, L. Wang, H. Zhou, C.A. Jimenez-Cruz, R. Zhou, The role of basic residues in the adsorption of blood proteins onto the graphene surface, Sci. Rep. 5 (2015) 10873.
[77] S.T. Yang, Y. Liu, Y.W. Wang, A. Cao, Biosafety and bioapplication of nanomaterials by designing protein-nanoparticle interactions, Small 9 (2013) 1635–1653.

[78] S. Tenzer, D. Docter, J. Kuharev, A. Musyanovych, V. Fetz, R. Hecht, F. Schlenk, D. Fischer, K. Kiouptsi, C. Reinhardt, K. Landfester, H. Schild, M. Maskos, S.K. Knauer, R.H. Stauber, Rapid formation of plasma protein corona critically affects nanoparticle pathophysiology, Nat. Nanotechnol. 8 (2013) 772–781.
[79] Z. Liu, J.T. Robinson, X.M. Sun, H.J. Dai, PEGylated nanographene oxide for delivery of water-insoluble cancer drugs, J. Am. Chem. Soc. 130 (2008) 10876 − +.
[80] W. Hu, C. Peng, M. Lv, X. Li, Y. Zhang, N. Chen, C. Fan, Q. Huang, Protein corona-mediated mitigation of cytotoxicity of graphene oxide, ACS Nano 5 (2011) 3693–3700.
[81] H.Y. Mao, W. Chen, S. Laurent, C. Thirifays, C. Burtea, F. Rezaee, M. Mahmoudi, Hard corona composition and cellular toxicities of the graphene sheets, Colloids Surf. B 109 (2013) 212–218.
[82] C. Cheng, S.Q. Nie, S. Li, H. Peng, H. Yang, L. Ma, S.D. Sun, C.S. Zhao, Biopolymer functionalized reduced graphene oxide with enhanced biocompatibility via mussel inspired coatings/anchors, J. Mater. Chem. B 1 (2013) 265–275.
[83] M. Papi, M.C. Lauriola, V. Palmieri, G. Ciasca, G. Maulucci, M. De Spirito, Plasma protein corona reduces the haemolytic activity of graphene oxide nano and micro flakes, RSC Adv. 5 (2015) 81638–81641.
[84] D.A. Mbeh, O. Akhavan, T. Javanbakht, M. Mahmoudi, L. Yahia, Cytotoxicity of protein corona-graphene oxide nanoribbons on human epithelial cells, Appl. Surf. Sci. 320 (2014) 596–601.
[85] M.J. Hajipour, J. Raheb, O. Akhavan, S. Arjmand, O. Mashinchian, M. Rahman, M. Abdolahad, V. Serpooshan, S. Laurent, M. Mahmoudi, Personalized disease-specific protein corona influences the therapeutic impact of graphene oxide, Nanoscale 7 (2015) 8978–8994.
[86] Z.X. Yang, C.C. Ge, J.J. Liu, Y. Chong, Z.L. Gu, C.A. Jimenez-Cruz, Z.F. Chai, R.H. Zhou, Destruction of amyloid fibrils by graphene through penetration and extraction of peptides, Nanoscale 7 (2015) 18725–18737.
[87] M. Orecchioni, D. Bedognetti, F. Sgarrella, F.M. Marincola, A. Bianco, L.G. Delogu, Impact of carbon nanotubes and graphene on immune cells, J. Transl. Med. 12 (2014) 138.
[88] H. Yue, W. Wei, Z. Yue, B. Wang, N. Luo, Y. Gao, D. Ma, G. Ma, Z. Su, The role of the lateral dimension of graphene oxide in the regulation of cellular responses, Biomaterials 33 (2012) 4013–4021.
[89] H. Zhou, K. Zhao, W. Li, N. Yang, Y. Liu, C. Chen, T. Wei, The interactions between pristine graphene and macrophages and the production of cytokines/chemokines via TLR- and NF-kappaB-related signaling pathways, Biomaterials 33 (2012) 6933–6942.
[90] G.Y. Chen, H.J. Yang, C.H. Lu, Y.C. Chao, S.M. Hwang, C.L. Chen, K.W. Lo, L.Y. Sung, W.Y. Luo, H.Y. Tuan, Y.C. Hu, Simultaneous induction of autophagy and toll-like receptor signaling pathways by graphene oxide, Biomaterials 33 (2012) 6559–6569.
[91] G. Qu, S. Liu, S. Zhang, L. Wang, X. Wang, B. Sun, N. Yin, X. Gao, T. Xia, J.J. Chen, G.B. Jiang, Graphene oxide induces toll-like receptor 4 (TLR4)-dependent necrosis in macrophages, ACS Nano 7 (2013) 5732–5745.
[92] C. Bussy, H. Ali-Boucetta, K. Kostarelos, Safety considerations for graphene: lessons learnt from carbon nanotubes, Acc. Chem. Res. 46 (2013) 692–701.
[93] J. Russier, E. Treossi, A. Scarsi, F. Perrozzi, H. Dumortier, L. Ottaviano, M. Meneghetti, V. Palermo, A. Bianco, Evidencing the mask effect of graphene oxide: a comparative study on primary human and murine phagocytic cells, Nanoscale 5 (2013) 11234–11247.
[94] A. Sasidharan, L.S. Panchakarla, A.R. Sadanandan, A. Ashokan, P. Chandran, C.M. Girish, D. Menon, S.V. Nair, C.N. Rao, M. Koyakutty, Hemocompatibility and macrophage response of pristine and functionalized graphene, Small 8 (2012) 1251–1263.
[95] X. Zhi, H.L. Fang, C.C. Bao, G.X. Shen, J.L. Zhang, K. Wang, S.W. Guo, T. Wan, D.X. Cui, The immunotoxicity of graphene oxides and the effect of PVP-coating, Biomaterials 34 (2013) 5254–5261.
[96] A.V. Tkach, N. Yanamala, S. Stanley, M.R. Shurin, G.V. Shurin, E.R. Kisin, A.R. Murray, S. Pareso, T. Khaliullin, G.P. Kotchey, V. Castranova, S. Mathur, B. Fadeel, A. Star, V.E. Kagan, A.A. Shvedova, Graphene oxide, but not fullerenes, targets immunoproteasomes and suppresses antigen presentation by dendritic cells, Small 9 (2013) 1686–1690.
[97] Y. Pan, N.G. Sahoo, L. Li, The application of graphene oxide in drug delivery, Expert Opin. Drug Deliv. 9 (2012) 1365–1376.
[98] K. Yang, S.A. Zhang, G.X. Zhang, X.M. Sun, S.T. Lee, Z.A. Liu, Graphene in mice: ultra-high in vivo tumor uptake and efficient photothermal therapy, Nano Lett. 10 (2010) 3318–3323.
[99] J.J. Shi, L. Wang, J. Zhang, R. Ma, J. Gao, Y. Liu, C.F. Zhang, Z.Z. Zhang, A tumor-targeting near-infrared laser-triggered drug delivery system based on GO@Ag nanoparticles for chemo-photothermal therapy and X-ray imaging, Biomaterials 35 (2014) 5847–5861.
[100] T.H. Kim, T. Lee, W.A. El-Said, J.W. Choi, Graphene-based materials for stem cell applications, Materials 8 (2015) 8674–8690.
[101] J. Park, Y.S. Kim, S. Ryu, W.S. Kang, S. Park, J. Han, H.C. Jeong, B.H. Hong, Y. Ahn, B.S. Kim, Graphene potentiates the myocardial repair efficacy of mesenchymal stem cells by stimulating the expression of angiogenic growth factors and gap junction protein, Adv. Funct. Mater. 25 (2015) 2590–2600.
[102] J. Park, B. Kim, J. Han, J. Oh, S. Park, S. Ryu, S. Jung, J.Y. Shin, B.S. Lee, B.H. Hong, D. Choi, B.S. Kim, Graphene oxide flakes as a cellular adhesive: prevention of reactive oxygen species mediated death of implanted cells for cardiac repair, ACS Nano 9 (2015) 4987–4999.
[103] S.K. Singh, M.K. Singh, P.P. Kulkarni, V.K. Sonkar, J.J. Gracio, D. Dash, Amine-modified graphene: thrombo-protective safer alternative to graphene oxide for biomedical applications, ACS Nano 6 (2012) 2731–2740.
[104] S. Jaworski, E. Sawosz, M. Kutwin, M. Wierzbicki, M. Hinzmann, M. Grodzik, A. Winnicka, L. Lipinska, K. Wlodyga, A. Chwalibog, In vitro and in vivo effects of graphene oxide and reduced graphene oxide on glioblastoma, Int. J. Nanomedicine 10 (2015) 1585–1596.
[105] E. Sawosz, S. Jaworski, M. Kutwin, K.P. Vadalasetty, M. Grodzik, M. Wierzbicki, N. Kurantowicz, B. Strojny, A. Hotowy, L. Lipinska, J. Jagiello, A. Chwalibog, Graphene functionalized with arginine decreases the development of glioblastoma multiforme tumor in a gene-dependent manner, Int. J. Mol. Sci. 16 (2015) 25214–25233.